Topology shapes dynamics of higher-order networks

Non-equilibrium statistical mechanics

Higgs Centre, Edinburgh

23 April 2025

Ginestra Bianconi

School of Mathematical Sciences, Queen Mary University of London
The Alan Turing Institute

Queen Mary University of London

Networks

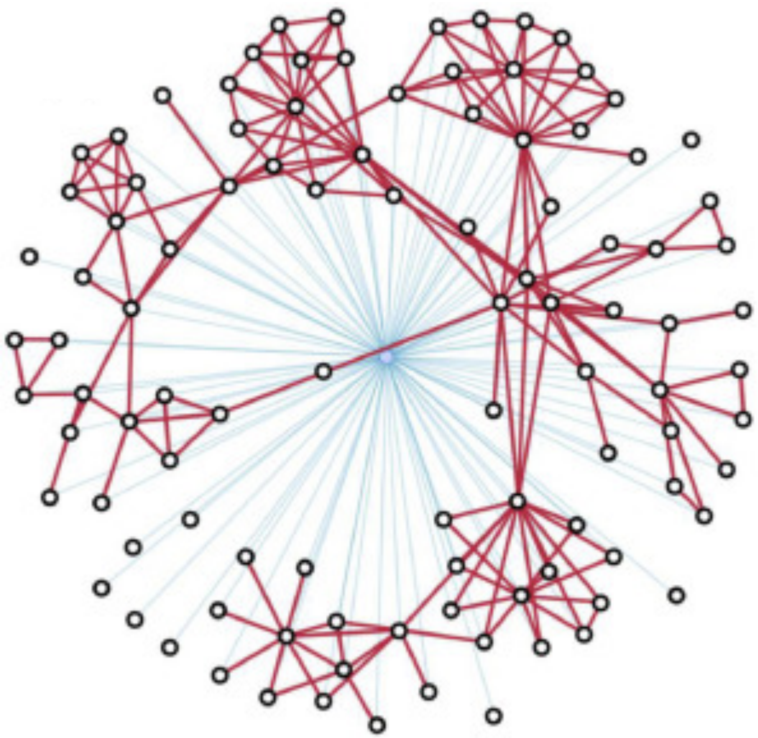

Simple network

Higher-order networks

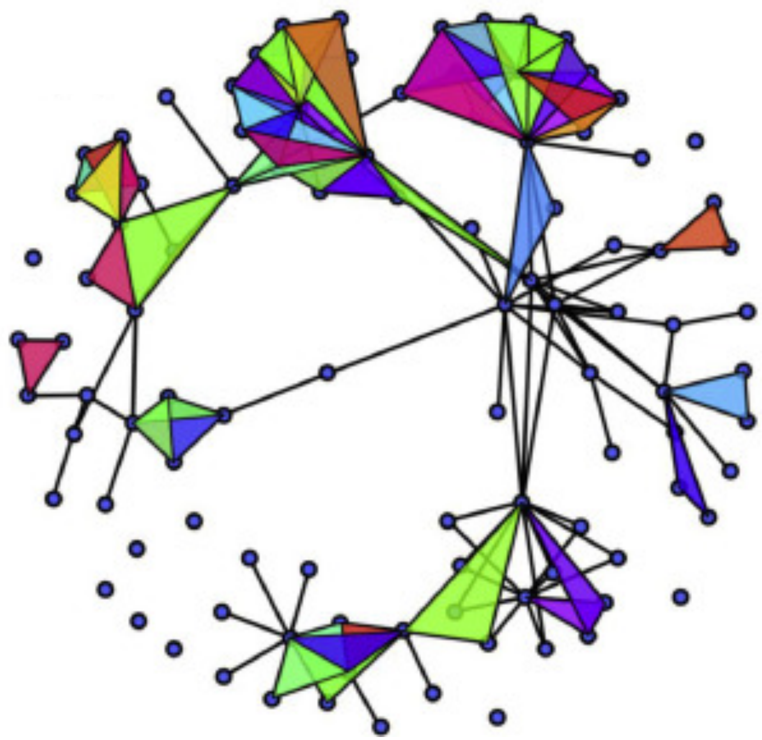

Simplicial complex

Higher order network

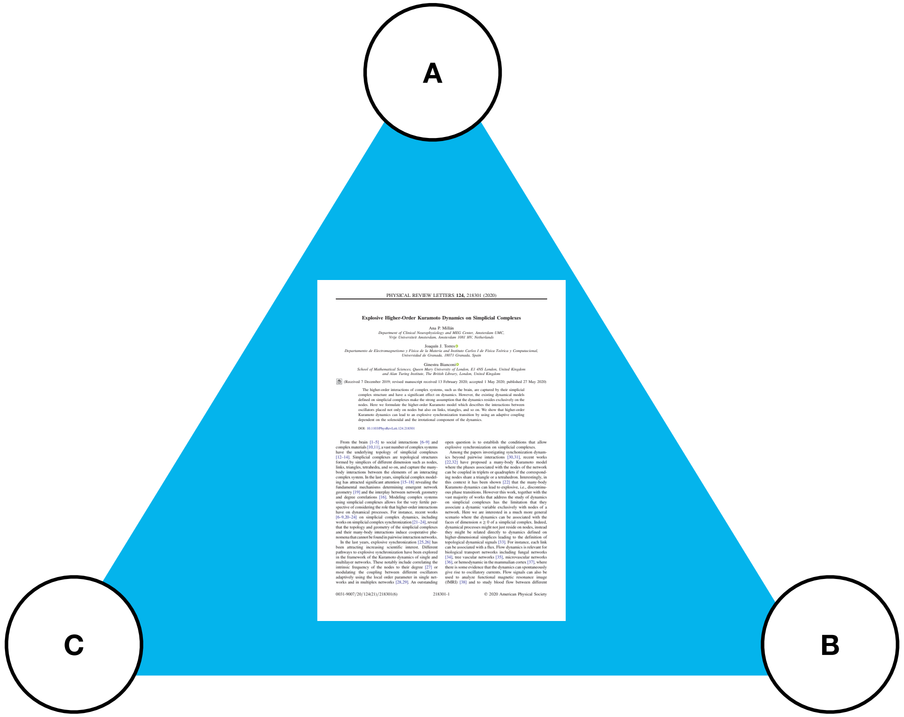

Collaboration network

Higher-order brain networks

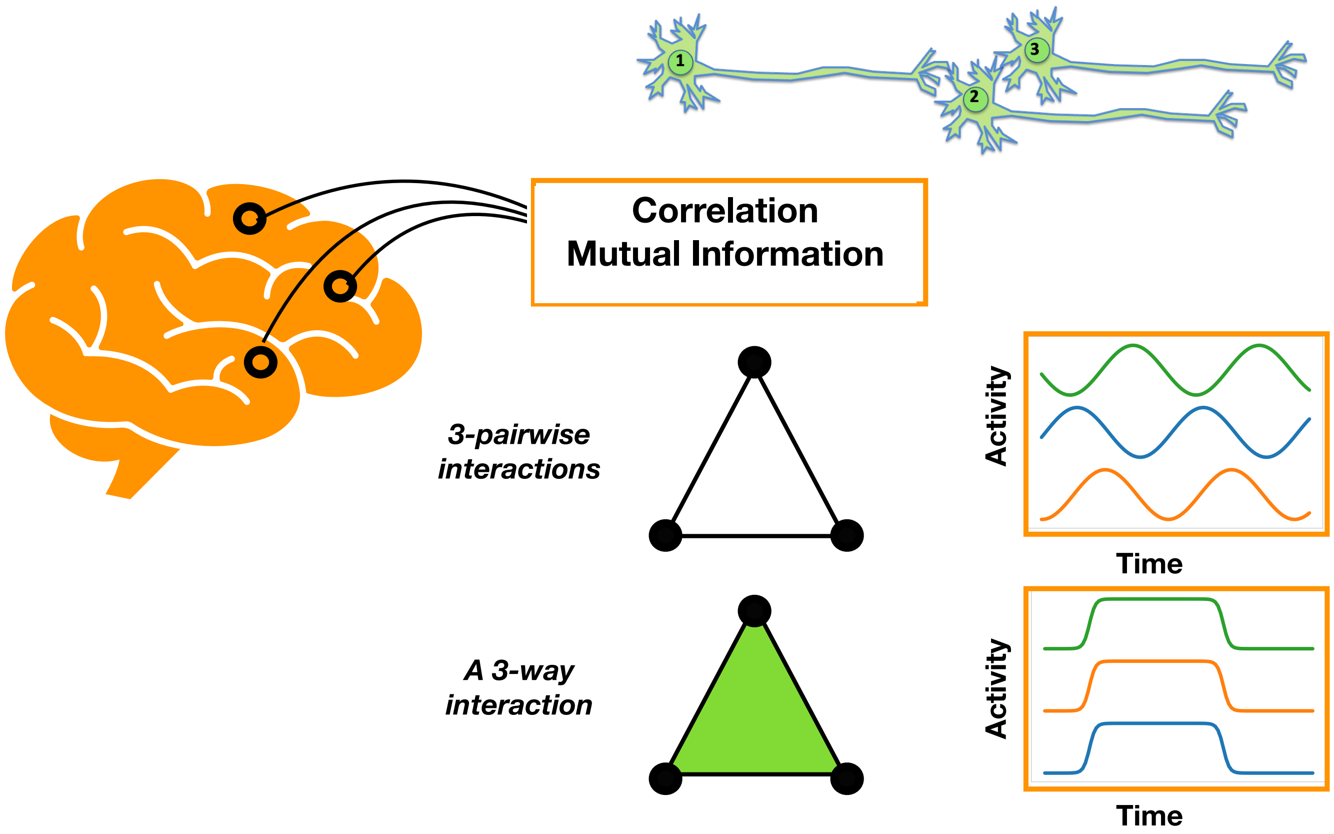

Triadic interactions

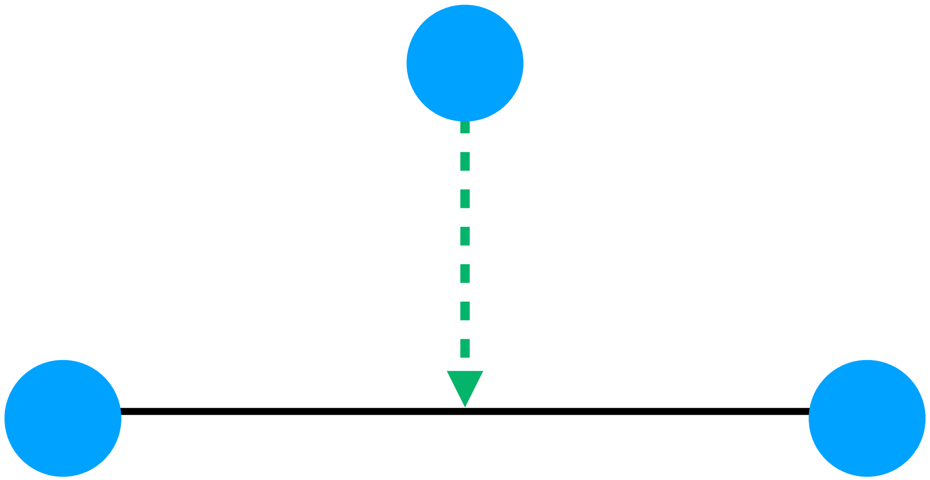

A triadic interaction occurs when a node affects the interaction between other two nodes

(Sun et. al Nature Communications 2023, Millan et al 2024, Sun 2024, Niedostatek 2024)

Triadic interactions
From neuroscience to triadic percolation

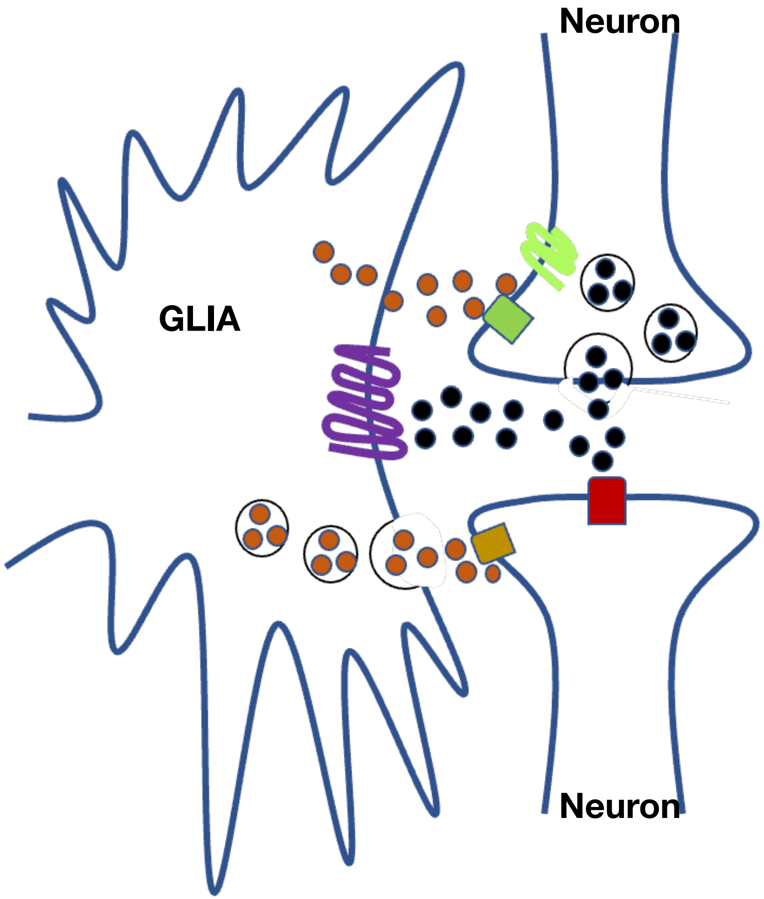

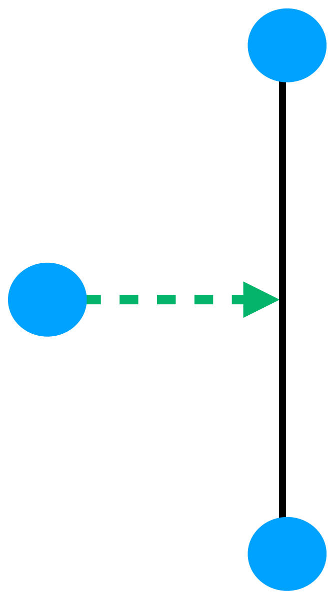

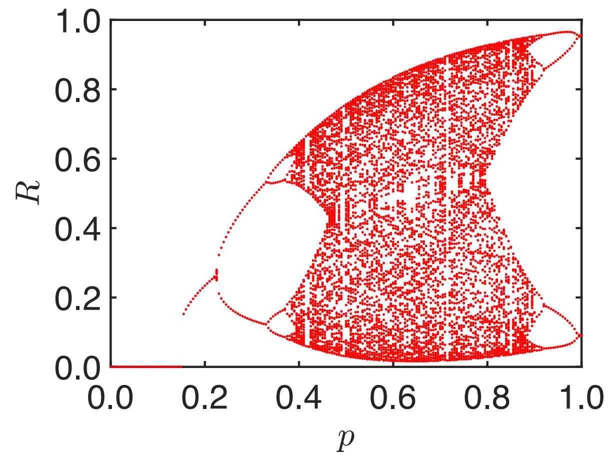

(Sun et. al Nature Communications 2023, Millan et al 2024)

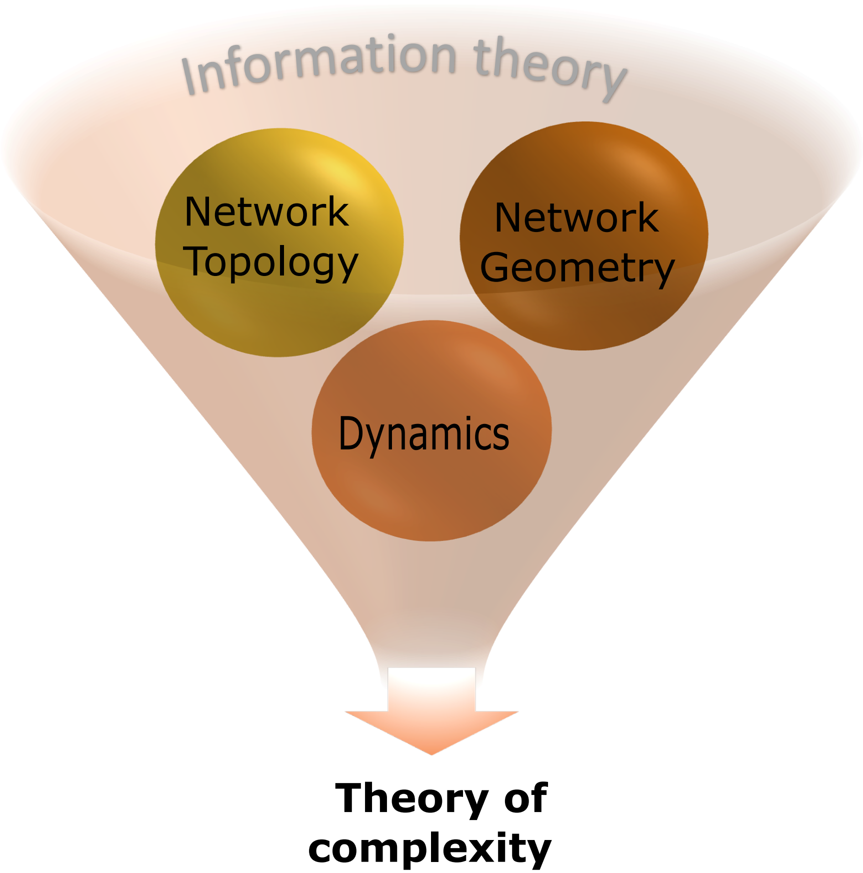

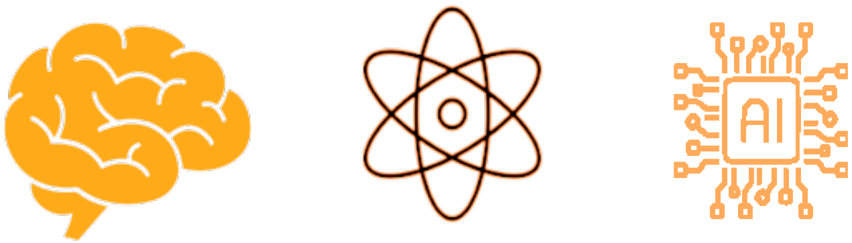

Complexity challenge

Simplicial complexes

Simplicial complexes are characterising the interactions between two ore more nodes and are formed by nodes, links, triangles, tetrahedra etc.

They allow for topological and geometrical interpretation of higher-order interactions

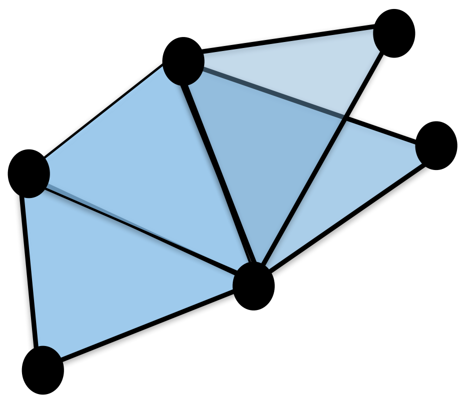

d=2 simplicial complex

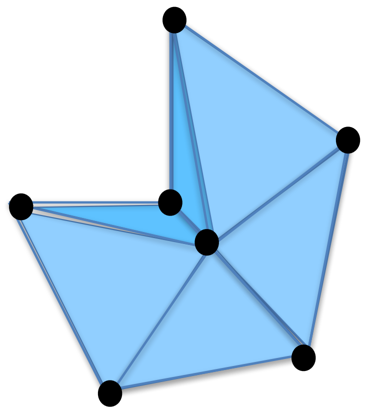

d=3 simplicial complex

Higher-order networks

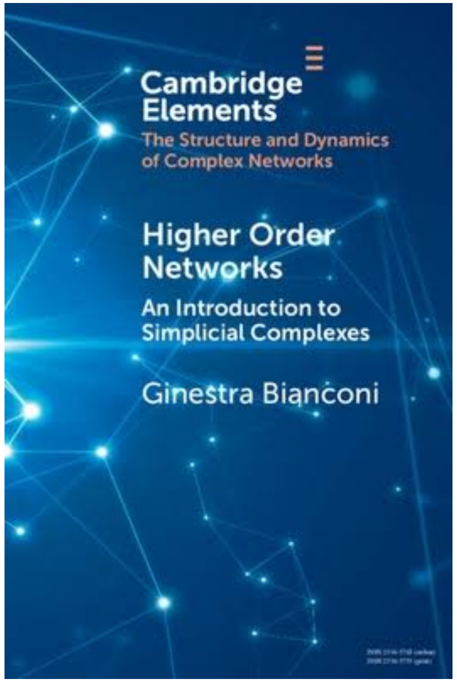

Book
by Cambridge University Press

Providing a general view of the interplay between topology and dynamics

Higher-order structure and dynamics

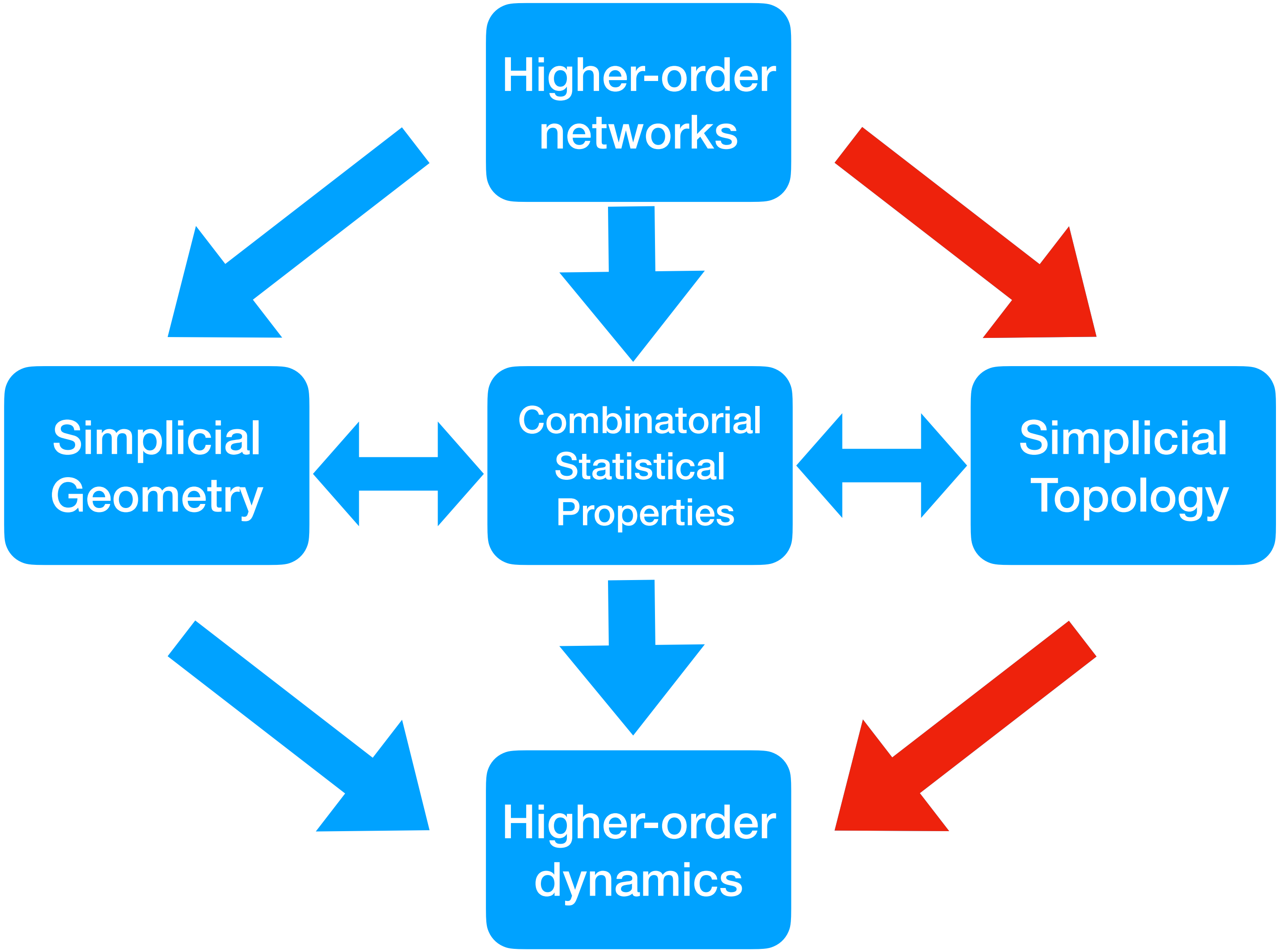

Simplicial complex models

Emergent Hyperbolic Geometry
Network Geometry with Flavor (NGF)
[Bianconi Rahmede ,2016 & 2017]

Maximum entropy model
Configuration model
of simplicial complexes
[Courtney Bianconi 2016]

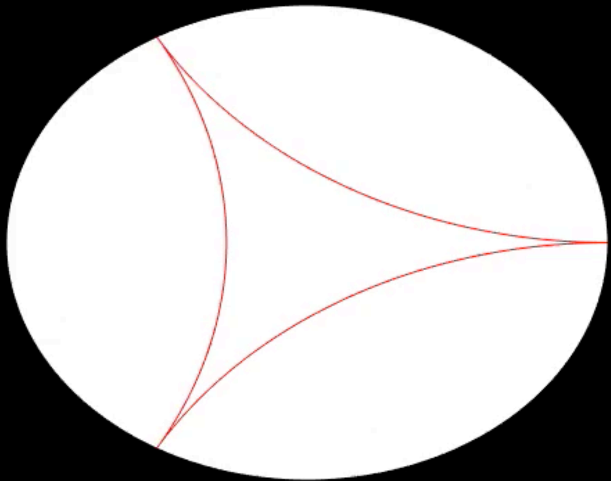

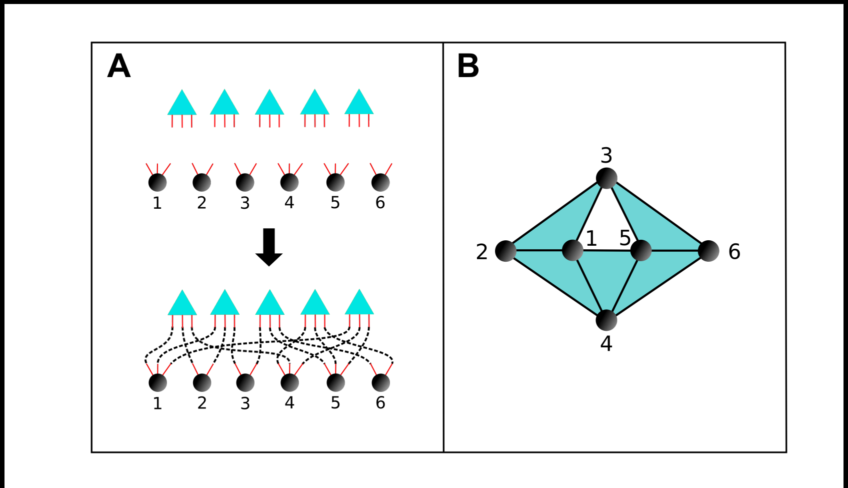

CODES AVAILABLE AT GITHUB ginestrab

Nature Physics Perspective

nature physics

Perspective https://doi.org/10.1038/s41567-024-02757-w

Topology shapes dynamics of higher-order networks

Received: 29 February 2024

Accepted: 6 December 2024

Published online: 19 February 2025

Check for updates

Ana P. Millán[1], Hanlin Sun[2], Lorenzo Giambagli[3,4], Riccardo Muolo[5], Timoteo Carletti[6], Joaquín J. Torres[1], Filippo Radicchi[7], Jürgen Kurths[8,9] & Ginestra Bianconi[10,11]

Higher-order networks capture the many-body interactions present in complex systems, shedding light on the interplay between topology and dynamics. The theory of higher-order topological dynamics, which

Topology and Betti numbers

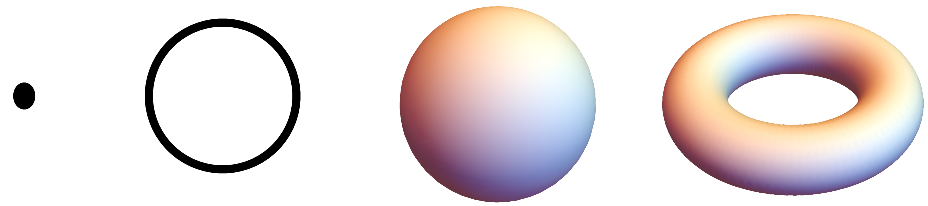

Point	Circle	Sphere	Torus
$\beta_0 = 1$	$\beta_0 = 1$	$\beta_0 = 1$	$\beta_0 = 1$
$\beta_1 = 0$	$\beta_1 = 1$	$\beta_1 = 0$	$\beta_1 = 2$
$\beta_2 = 0$	$\beta_2 = 0$	$\beta_2 = 1$	$\beta_2 = 1$

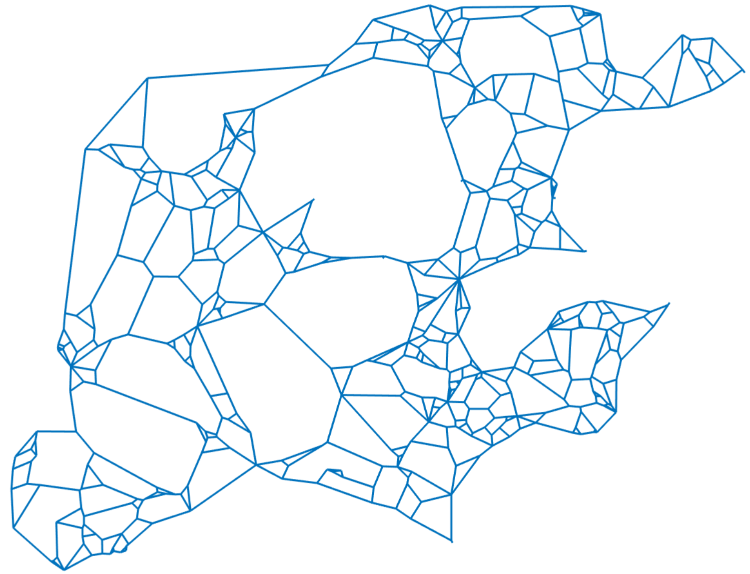

Fungi network from
Sang Hoon Lee, et. al. Jour. Compl. Net. (2016)

Topological signals

Beyond the node centered description of network dynamics
The dynamical state of a simplicial complex includes
node, edge, and higher-order topological signals

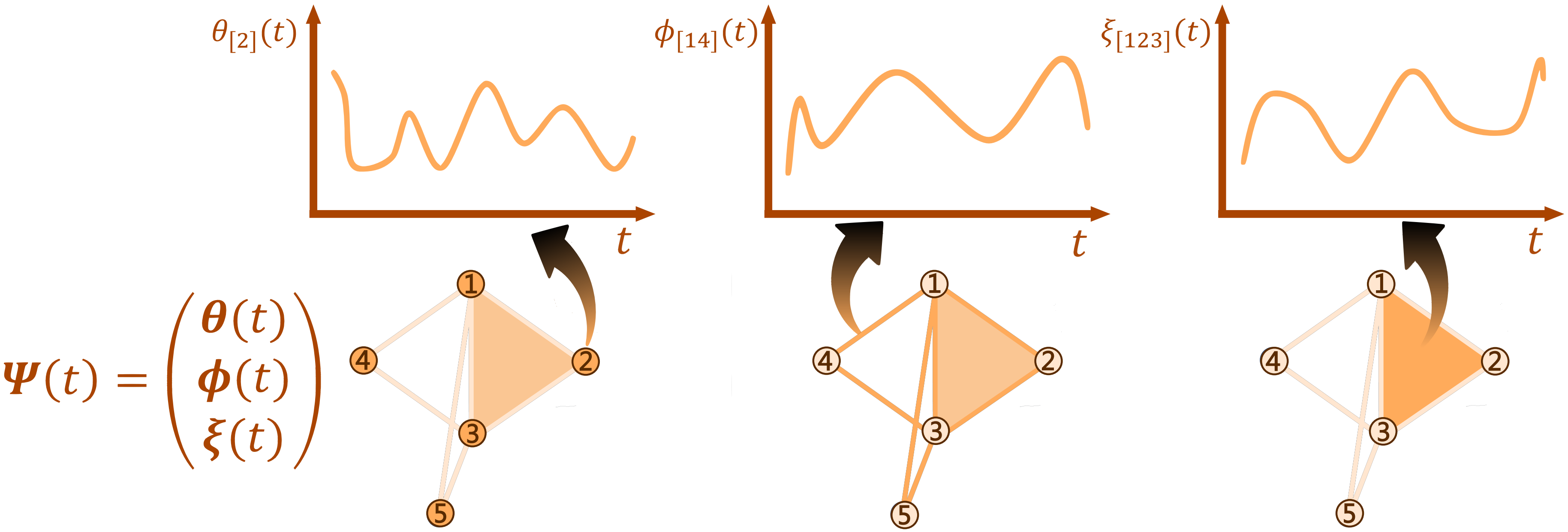

Topological signals

Topological signals are not only defined on nodes but also on links, triangles and higher-order simplices

- Synaptic signal
- Edge signals in the brain
- Citations in a collaboration network
- Speed of wind at given locations
- Currents at given locations in the ocean
- Fluxes in biological transportation networks

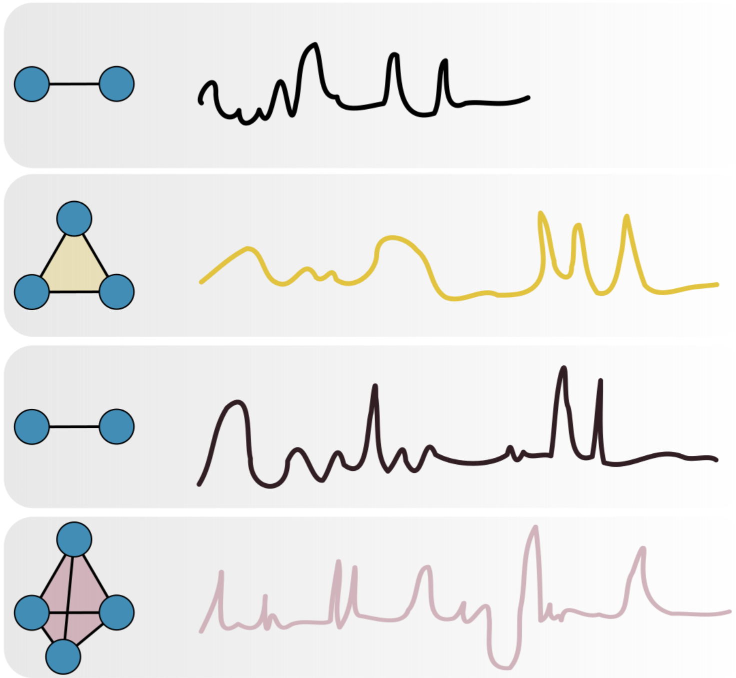

Battiston et al. The physics of higher-order interactions in complex systems Nature Physics 2021

Dynamical state of a higher-order network

The dynamical state on a higher order network

formed by nodes, edges and triangles is defined by a topological spinor

$$\mathbf{\Psi} = \begin{pmatrix} \boldsymbol{\chi} \\ \boldsymbol{\psi} \\ \boldsymbol{\xi} \end{pmatrix}$$

with

$\boldsymbol{\chi}$ defined on nodes, $\boldsymbol{\chi} \in C^0$, $\boldsymbol{\psi}$ defined on edges, $\boldsymbol{\psi} \in C^1$

$\boldsymbol{\xi}$ defined on triangles, i.e. $\boldsymbol{\xi} \in C^2$

Discrete exterior calculus

- The 0th order coboundary operator $\delta_0 : C^0 \to C^1$ is defined as

$$(\delta_0 \chi)_{e=[i,j]} = \chi_j - \chi_i \quad \textbf{gradient}$$

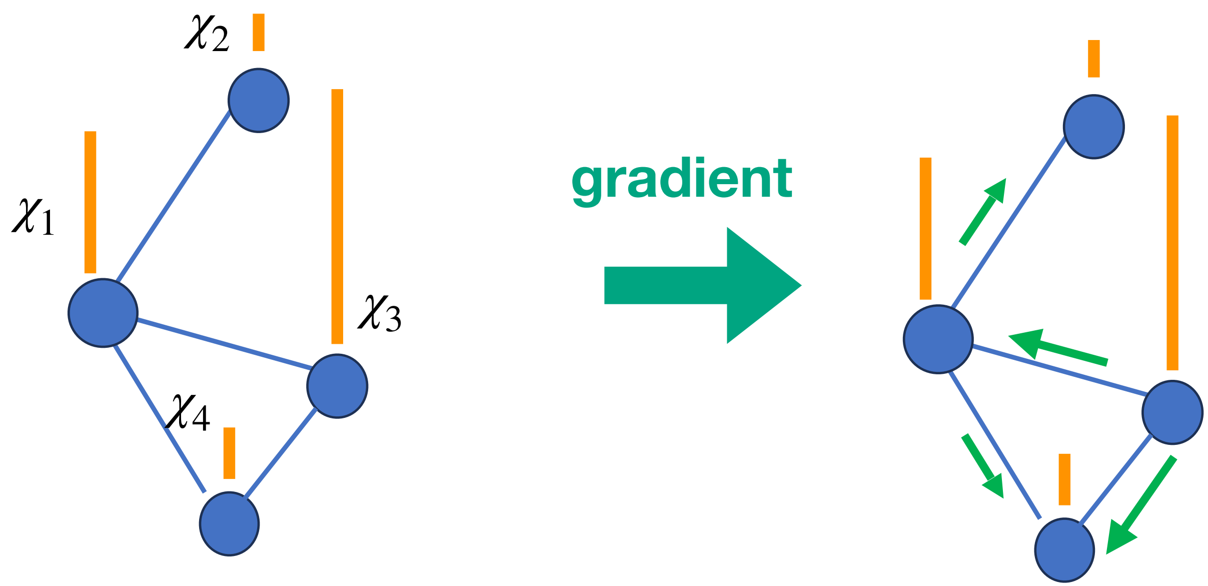

Discrete exterior calculus

- It adjoint operator $\delta_0^* : C^1 \to C^0$ is defined as

$$(\delta_0^* \psi)_i = \sum_{e \in E_i^+} \psi_e - \sum_{e \in E_i^-} \psi_e$$ **divergence**

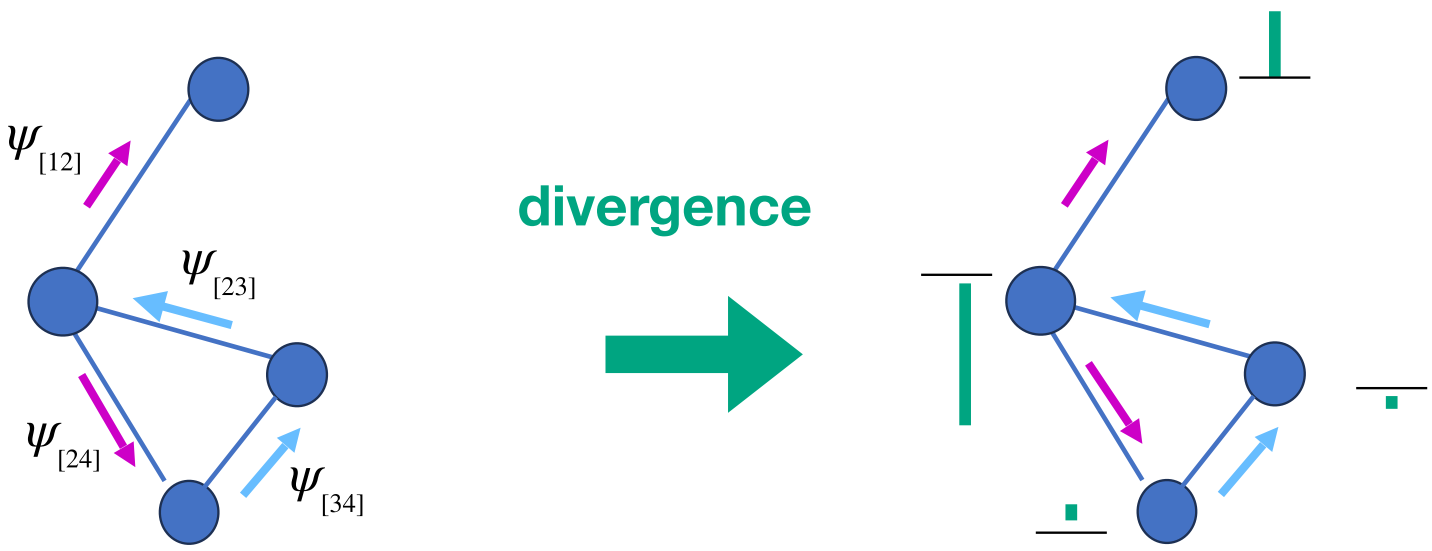

Discrete exterior calculus

- The 1st order coboundary operator $\delta_1^* : C^1 \rightarrow C^2$ is defined as

$$(\delta_1^* \boldsymbol{\psi})_{ijk} = \psi_{ij} + \psi_{jk} - \psi_{ik} \text{ curl}$$

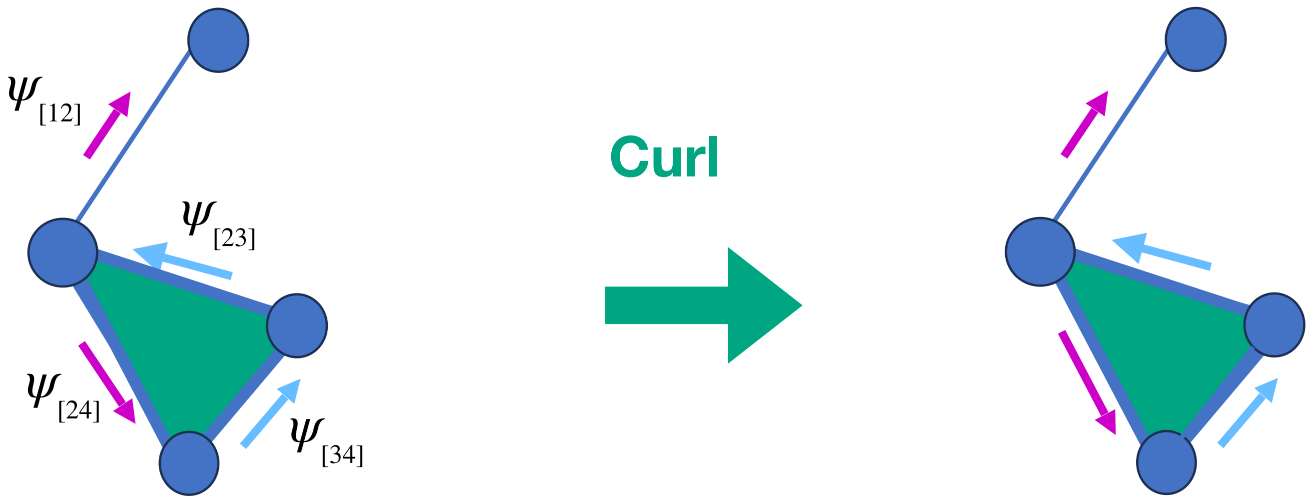

Basics of Algebraic Topology: the boundary operators

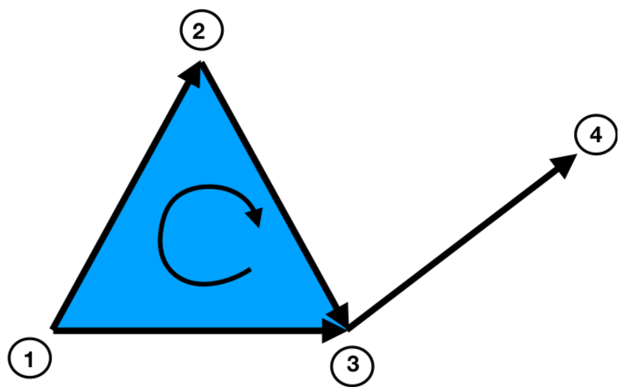

Boundary operators

$$\mathbf{B}_{[1]} = \begin{array}{c} \\ [1] \\ [2] \\ [3] \\ [4] \end{array} \begin{array}{cccc} [1,2] & [1,3] & [2,3] & [3,4] \\ -1 & -1 & 0 & 0 \\ 1 & 0 & -1 & 0 \\ 0 & 1 & 1 & -1 \\ 0 & 0 & 0 & 1 \end{array}, \qquad \mathbf{B}_{[2]} = \begin{array}{c} \\ [1,2] \\ [1,3] \\ [2,3] \\ [3,4] \end{array} \begin{array}{c} [1,2,3] \\ 1 \\ -1 \\ 1 \\ 0 \end{array}.$$

The boundary of the boundary is null

$$\mathbf{B}_{[n-1]}\mathbf{B}_{[n]} = \mathbf{0}, \quad \mathbf{B}_{[n]}^{\top}\mathbf{B}_{[n-1]}^{\top} = \mathbf{0}$$

$\mathbf{B}_{[1]}$ **Discrete divergence**

$\mathbf{B}_{[1]}^{\top}$ **Discrete gradient**

$\mathbf{B}_{[2]}^{\top}$ **Discrete Curl**

Simplicial complexes and Hodge Laplacians

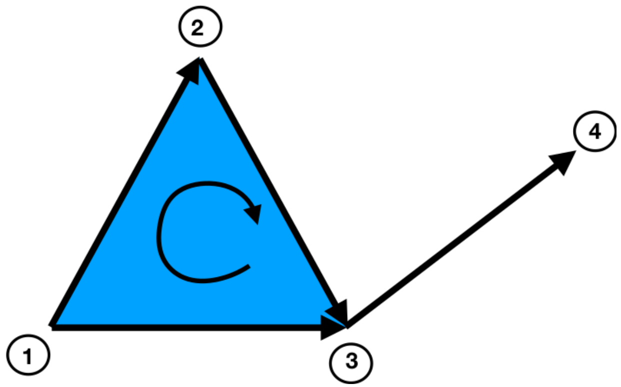

Hodge Laplacians

The Hodge Laplacians describe higher-order diffusion

e.g. the 1-Hodge Laplacian describes diffusion from edges to edge

through nodes or through triangles

$$\mathbf{L}_{[n]} = \mathbf{B}_{[n]}^{\top}\mathbf{B}_{[n]} + \mathbf{B}_{[n+1]}\mathbf{B}_{[n+1]}^{\top}$$

The dimension of the kernel of the Hodge Laplacian $\mathbf{L}_{[n]}$ is given by the n Betti number β_n

Harmonic eigenvectors of the graph Laplacian

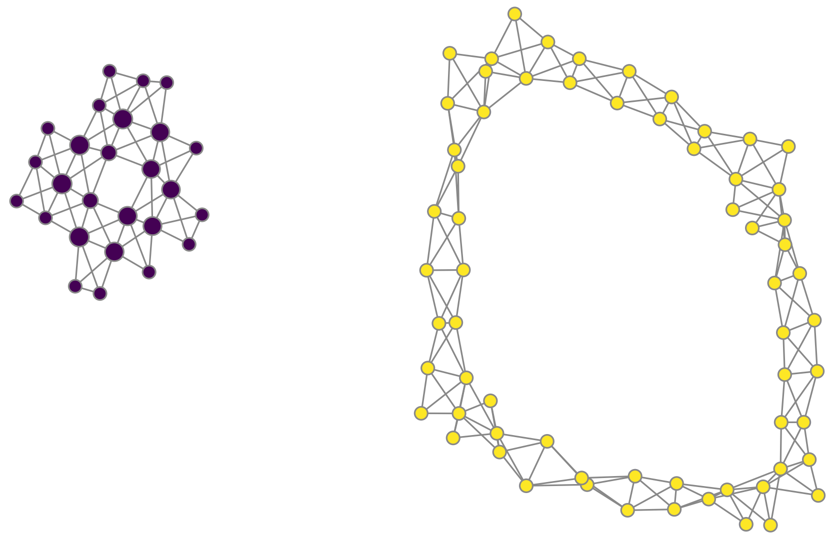

The graph Laplacian

$$\mathbf{L}_{[0]} = \mathbf{B}_{[1]}\mathbf{B}_{[1]}^{\top} = \mathbf{K} - \mathbf{A}$$

The harmonic eigenvectors of the graph Laplacian are constant on each connected component of the graph.

Higher-order harmonic eigenvectors

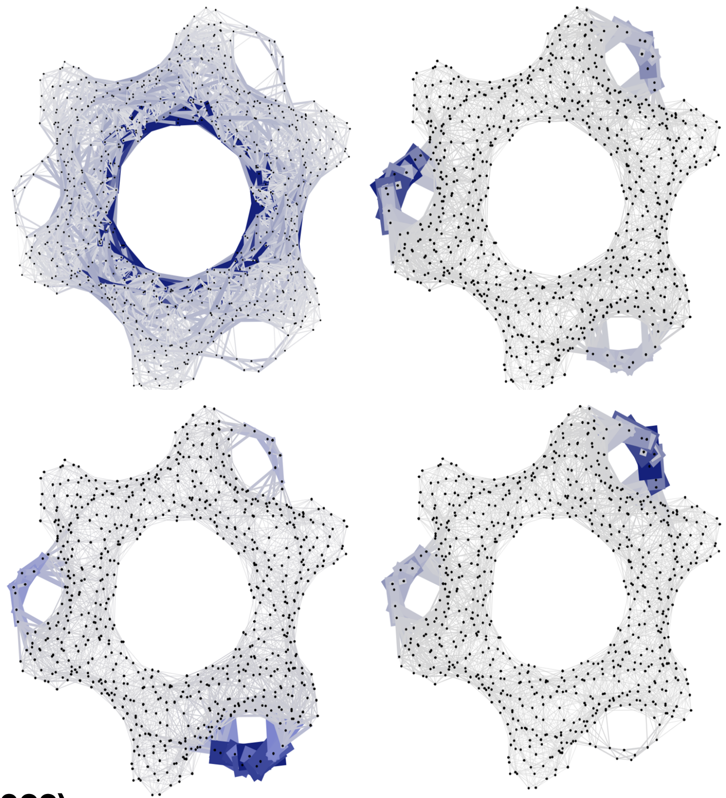

Wee et al. (2023)

The harmonic eigevectors of the higher-order Hodge Laplacian $\mathbf{L}_{[n]}$ are determined by the homology of the simplicial complex

There is a basis in which they localise along the holes of the simplicial complex

Hodge decomposition

The Hodge decomposition implies that topological signals can be decomposed

in a irrotational, harmonic and solenoidal components

$$\boxed{\mathbb{R}^{D_n} = \textbf{im}(\mathbf{B}_{[n]}^{\top}) \oplus \textbf{ker}(\mathbf{L}_{[n]}) \oplus \textbf{im}(\mathbf{B}_{[n+1]})}$$

which in the case of topological signals of the links can be decomposed as

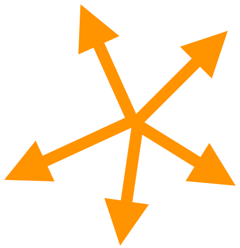

Irrotational component
Gradient Flow

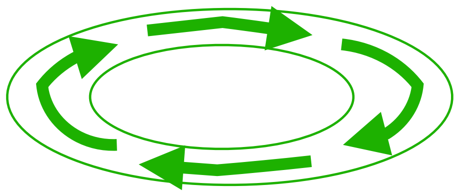

Harmonic component

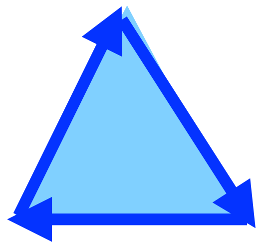

Solenoidal component
Curl Flow

Topology and Dynamics

Synchronization on a network

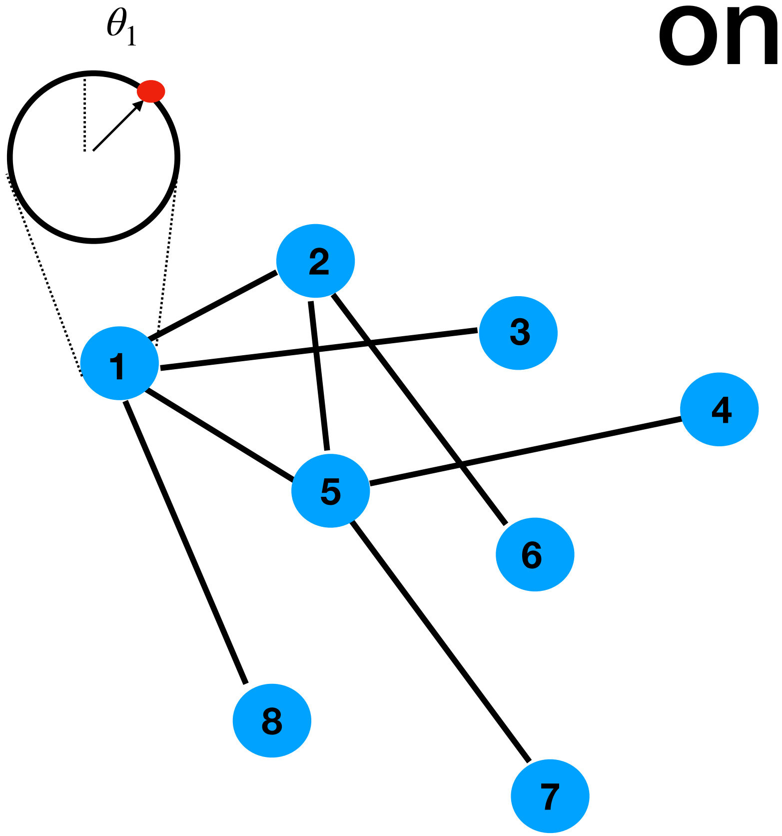

The Kuramoto model

$$\dot{\theta}_r = \omega_r + \sigma \sum_{j=1}^{N} a_{rj} \sin\left(\theta_j - \theta_r\right) \qquad \textbf{With} \qquad \omega \sim \mathcal{N}(\Omega, 1)$$

describes synchronization of node phases of $\sigma > \sigma_c$

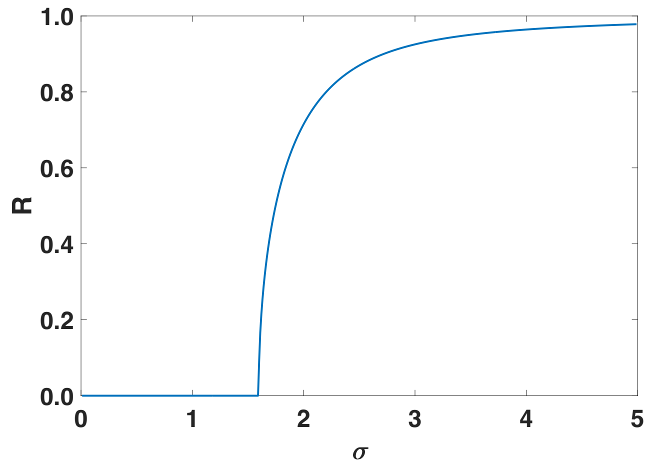

Order parameter

$$R = \frac{1}{N} \left| \sum_{r=1}^{N} e^{i\theta_r} \right|$$

The Topological Kuramoto model

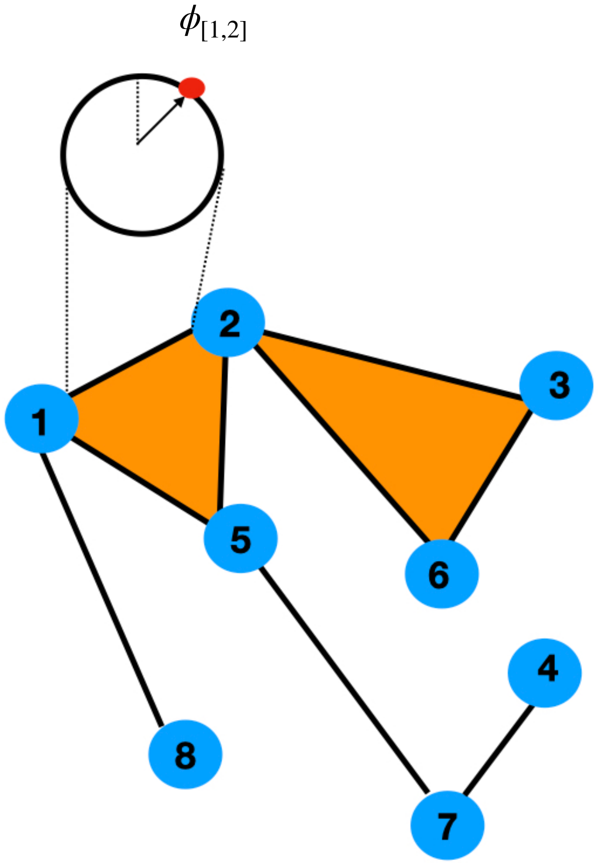

How to define
the Topological Higher-order Kuramoto model
coupling higher dimensional
topological signals?

A. P. Millan, J.J. Torres and G. Bianconi PRL (2020)

Topological Kuramoto model

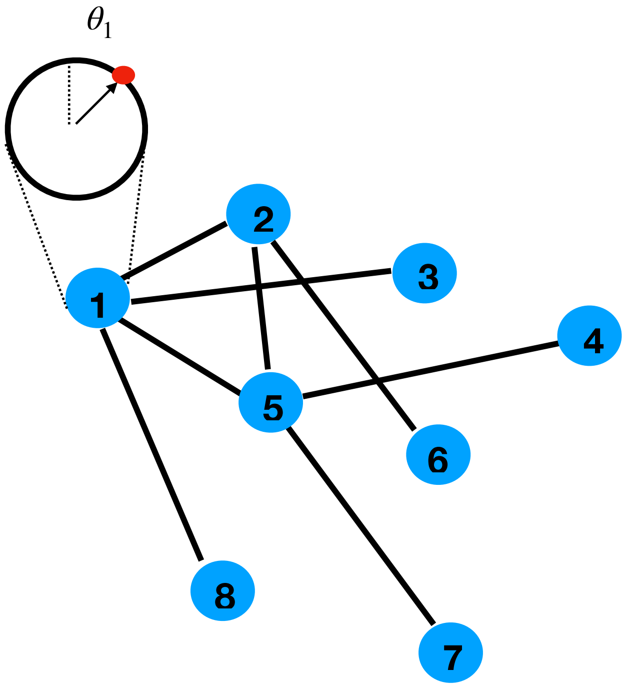

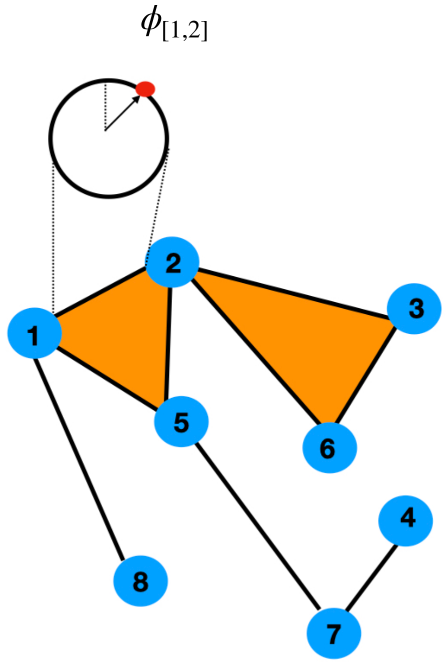

Standard Kuramoto model

$$\dot{\boldsymbol{\theta}} = \boldsymbol{\omega} - \sigma \mathbf{B}_{[1]} \sin \mathbf{B}_{[1]}^{\top} \boldsymbol{\theta}$$

Topological Higher-order Kuramoto model

$$\dot{\boldsymbol{\phi}} = \hat{\boldsymbol{\omega}} - \sigma \mathbf{B}_{[n+1]} \sin \mathbf{B}_{[n+1]}^{\top} \boldsymbol{\phi} - \sigma \mathbf{B}_{[n]}^{\top} \sin \mathbf{B}_{[n]} \boldsymbol{\phi},$$

A. P. Millan, J.J. Torres and G. Bianconi PRL (2020)

The Kuramoto model for node signals

Standard Kuramoto model

$$\dot{\boldsymbol{\theta}} = \boldsymbol{\omega} - \sigma \mathbf{B}_{[1]} \sin \mathbf{B}_{[1]}^{\top} \boldsymbol{\theta}$$

In the Standard Kuramoto model the free dynamics is along the harmonic eigenvector of the graph Laplacian

$$\frac{d\langle \mathbf{u}_{harm}, \boldsymbol{\theta} \rangle}{dt} = \langle \mathbf{u}_{harm}, \boldsymbol{\omega} \rangle$$

The free dynamics is uniform on each connected component

The Topological Kuramoto model

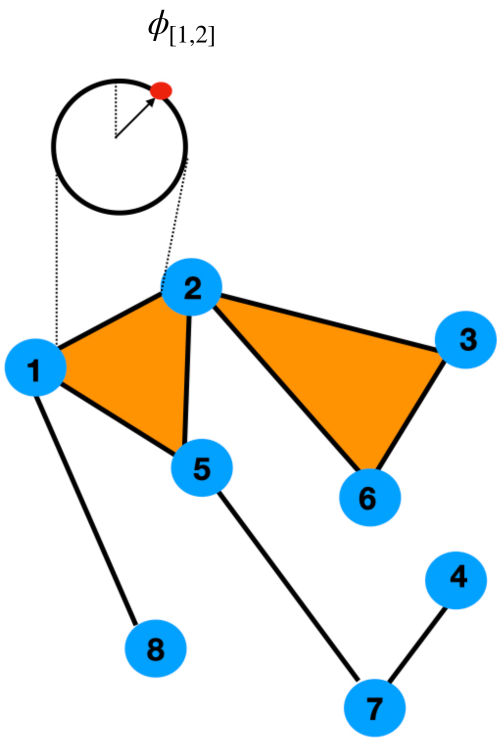

Topological Higher-order Kuramoto model

$$\dot{\boldsymbol{\phi}} = \hat{\omega} - \sigma \mathbf{B}_{[n+1]} \sin \mathbf{B}_{[n+1]}^{\top} \boldsymbol{\phi} - \sigma \mathbf{B}_{[n]}^{\top} \sin \mathbf{B}_{[n]} \boldsymbol{\phi},$$

In the Topological Kuramoto model the free dynamics is localised on the n-dimensional holes

$$\frac{d\langle \mathbf{u}_{harm}, \boldsymbol{\phi} \rangle}{dt} = \langle \mathbf{u}_{harm}, \hat{\boldsymbol{\omega}} \rangle$$

The free dynamics is localised on harmonic components

A. P. Millan, J.J. Torres and G. Bianconi PRL (2020)

Hamiltonian of the Topological Kuramoto model

The Topological Kuramoto is an Hamiltonian gradient flow

Hamiltonian of the Standard Kuramoto model (XY model)

$$H = -\boldsymbol{\omega}^\top \boldsymbol{\theta} - \sigma \mathbf{1}^\top \cos(\mathbf{B}_{[1]}^\top \boldsymbol{\theta})$$

$$= -\sum_{i=1}^{N} \omega_i \theta_i - \sigma \sum_{<i,j>} \cos(\theta_j - \theta_i)$$

Hamiltonian of the Topological Kuramoto model

$$H = -\hat{\boldsymbol{\omega}}^\top \boldsymbol{\phi} - \sigma \mathbf{1}^\top \cos(\mathbf{B}_{[n]} \boldsymbol{\phi}) - \sigma \mathbf{1}^\top \cos(\mathbf{B}_{[n+1]}^\top \boldsymbol{\phi})$$

Topological Synchronisation

The dynamical ordered state has many minima
Each corresponding to a single homology class of the simplicial complex (hole)

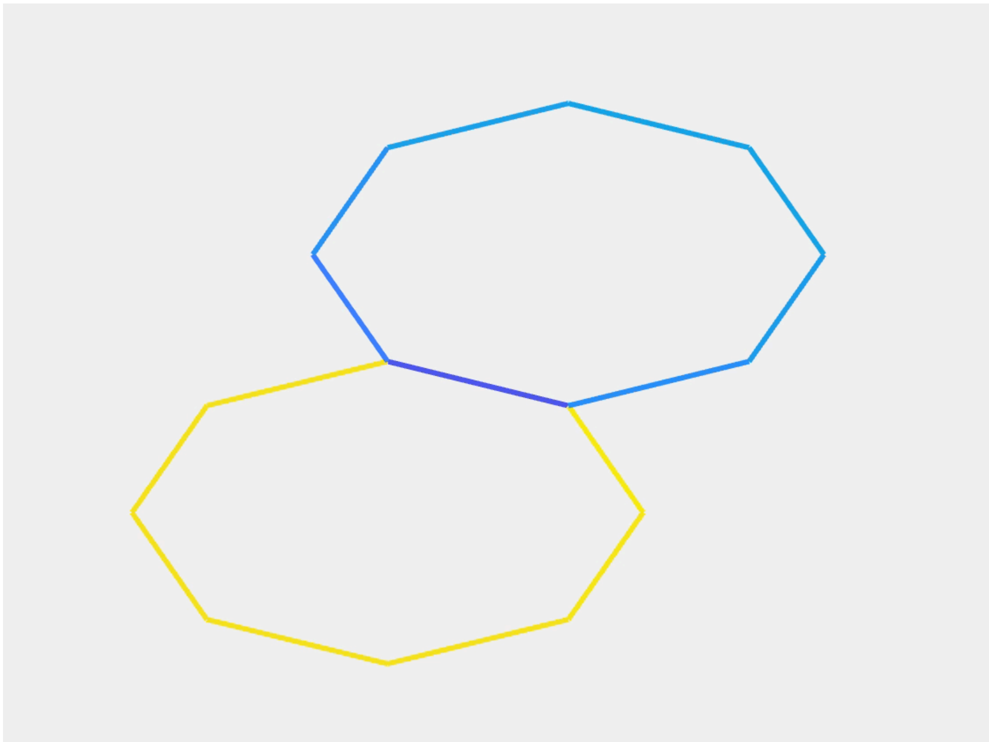

Topology shapes dynamics

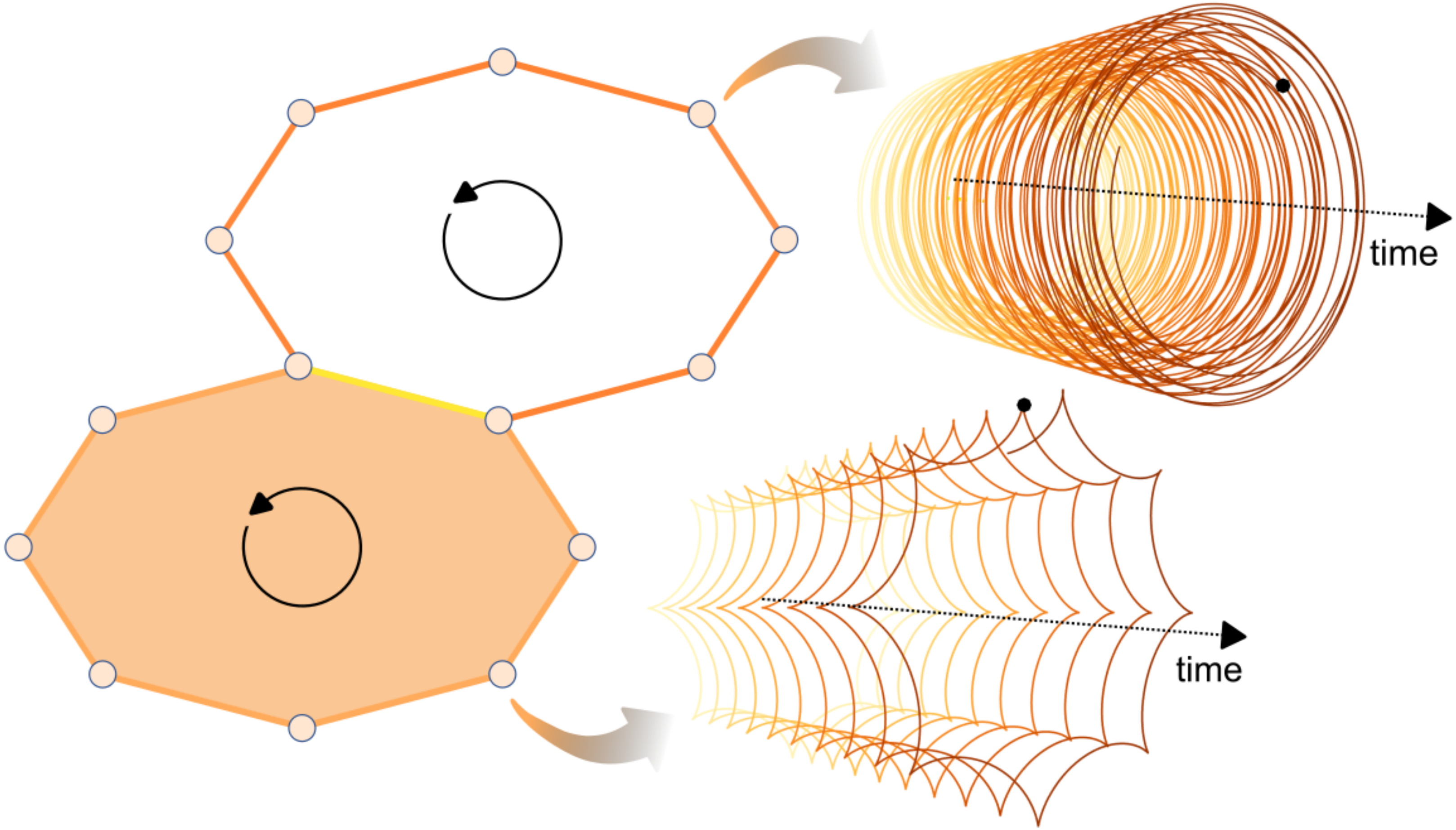

Higher-order synchronization transition

Emergence of order
We project the signal one dimension up
or one dimension down
If we have a signal of the links
we project the signal on nodes and triangles

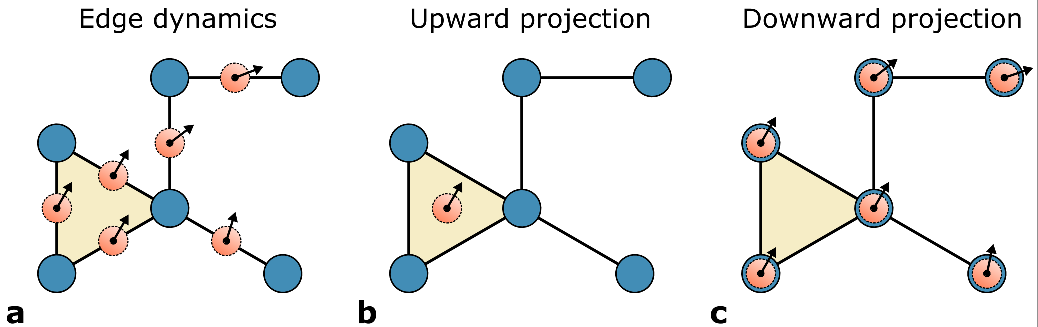

$\boldsymbol{\phi}$ $\quad\quad$ $\boldsymbol{\phi}^{[+]} = \mathbf{B}_{[n+1]}^{\top}\boldsymbol{\phi}$ $\quad\quad$ $\boldsymbol{\phi}^{[-]} = \mathbf{B}_{[n]}\boldsymbol{\phi}$

Topological Higher-order Kuramoto model

$$\dot{\boldsymbol{\phi}} = \hat{\boldsymbol{\omega}} - \sigma\mathbf{B}_{[n+1]}\sin\mathbf{B}_{[n+1]}^{\top}\boldsymbol{\phi} - \sigma\mathbf{B}_{[n]}^{\top}\sin\mathbf{B}_{[n]}\boldsymbol{\phi},$$

Projected dynamics

$$\dot{\boldsymbol{\phi}}^{[+]} = \mathbf{B}_{[n+1]}^{\top}\hat{\boldsymbol{\omega}} - \sigma\mathbf{L}_{[n+1]}^{[down]}\sin(\boldsymbol{\phi}^{[+]})$$
$$\dot{\boldsymbol{\phi}}^{[-]} = \mathbf{B}_{[n]}\hat{\boldsymbol{\omega}} - \sigma\mathbf{L}_{[n-1]}^{[up]}\sin(\boldsymbol{\phi}^{[-]})$$

Higher-order synchronization transition

Order parameters of topological synchronisation

$$R^{[+]} = \frac{1}{N_{n+1}} \left| \sum_{\alpha=1}^{N_{n+1}} e^{\phi_\alpha^{[+]}} \right| \qquad R^{[-]} = \frac{1}{N_{n-1}} \left| \sum_{\alpha=1}^{N_{n-1}} e^{\phi_\alpha^{[-]}} \right|$$

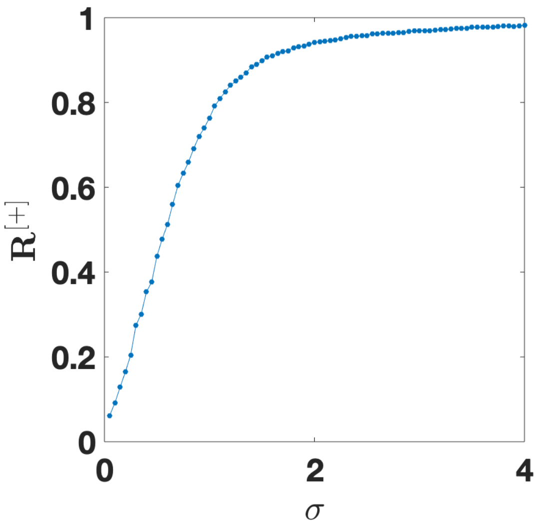

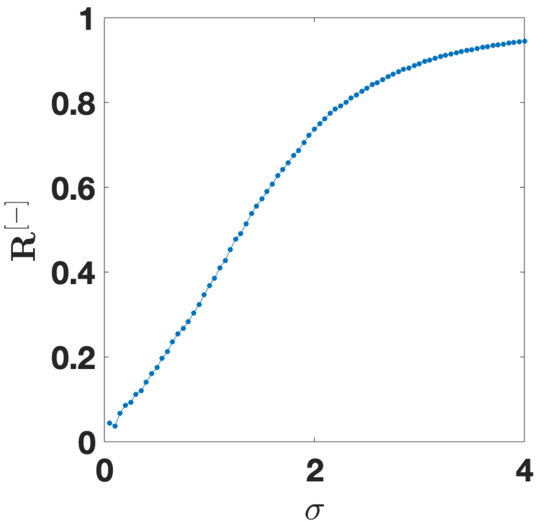

Explosive higher-order Kuramoto model

Adaptive global coupling

$$\dot{\boldsymbol{\phi}} = \hat{\boldsymbol{\omega}} - \sigma R^{[-]} \mathbf{B}_{[n+1]} \sin \mathbf{B}_{[n+1]}^{\top} \boldsymbol{\phi} - \sigma R^{[+]} \mathbf{B}_{[n]}^{\top} \sin \mathbf{B}_{[n]} \boldsymbol{\phi}$$

Coupled projected dynamics

$$\dot{\boldsymbol{\phi}}^{[+]} = \mathbf{B}_{[n+1]}^{\top} \hat{\boldsymbol{\omega}} - \sigma R^{[-]} \mathbf{L}_{[n+1]}^{[down]} \sin(\boldsymbol{\phi}^{[+]})$$

$$\dot{\boldsymbol{\phi}}^{[-]} = \mathbf{B}_{[n]} \hat{\boldsymbol{\omega}} - \sigma R^{[+]} \mathbf{L}_{[n-1]}^{[up]} \sin(\boldsymbol{\phi}^{[-]})$$

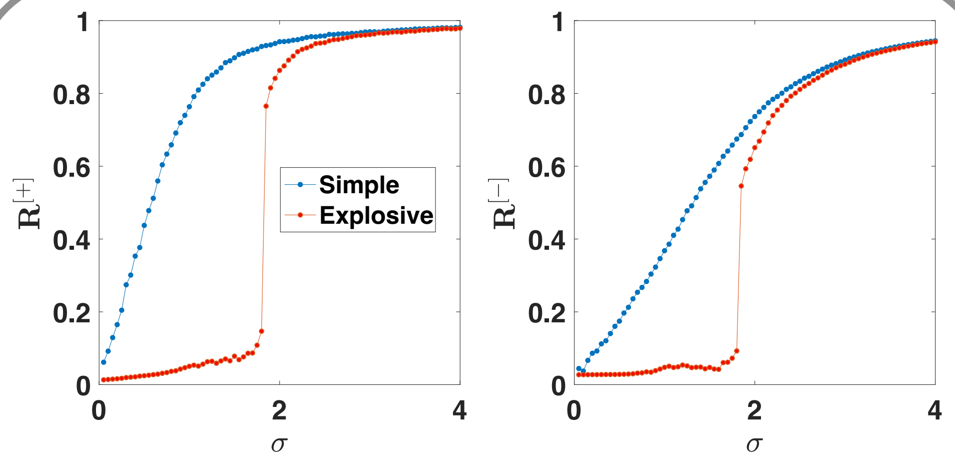

Higher-order synchronisation on real Connectomes

Homo sapiens Connectome

C.elegans Connectome

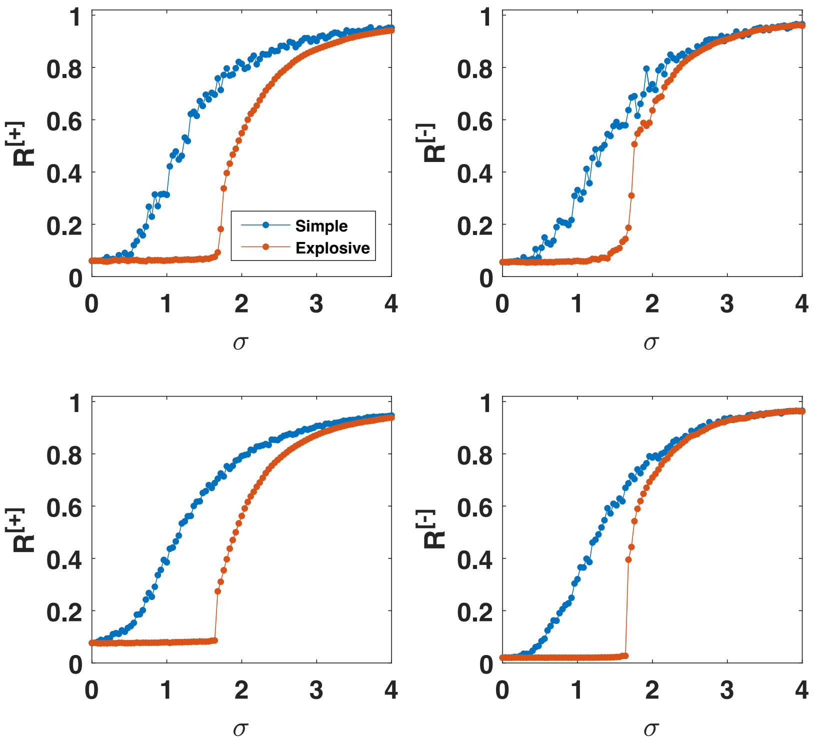

Analytical predictions of discontinuous transition on networks

$$\dot{\boldsymbol{\theta}} = \boldsymbol{\omega} - \sigma R_1^{[-]} \mathbf{B}_{[1]} \sin \mathbf{B}_{[1]}^\top \boldsymbol{\theta}$$

$$\dot{\boldsymbol{\phi}} = \hat{\boldsymbol{\omega}} - \sigma R_0 \mathbf{B}_{[n]}^\top \sin \mathbf{B}_{[n]} \boldsymbol{\phi}$$

The annealed solution reveals that the transition is discontinuous

Poisson network

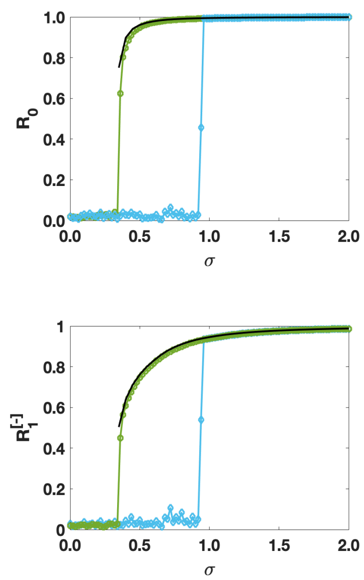

Scale-free network

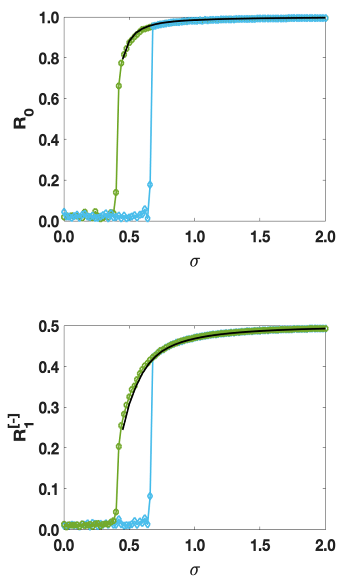

R. Ghorbanchian, Torres, Restrepo, Bianconi (2021)

Global Topological Synchronization

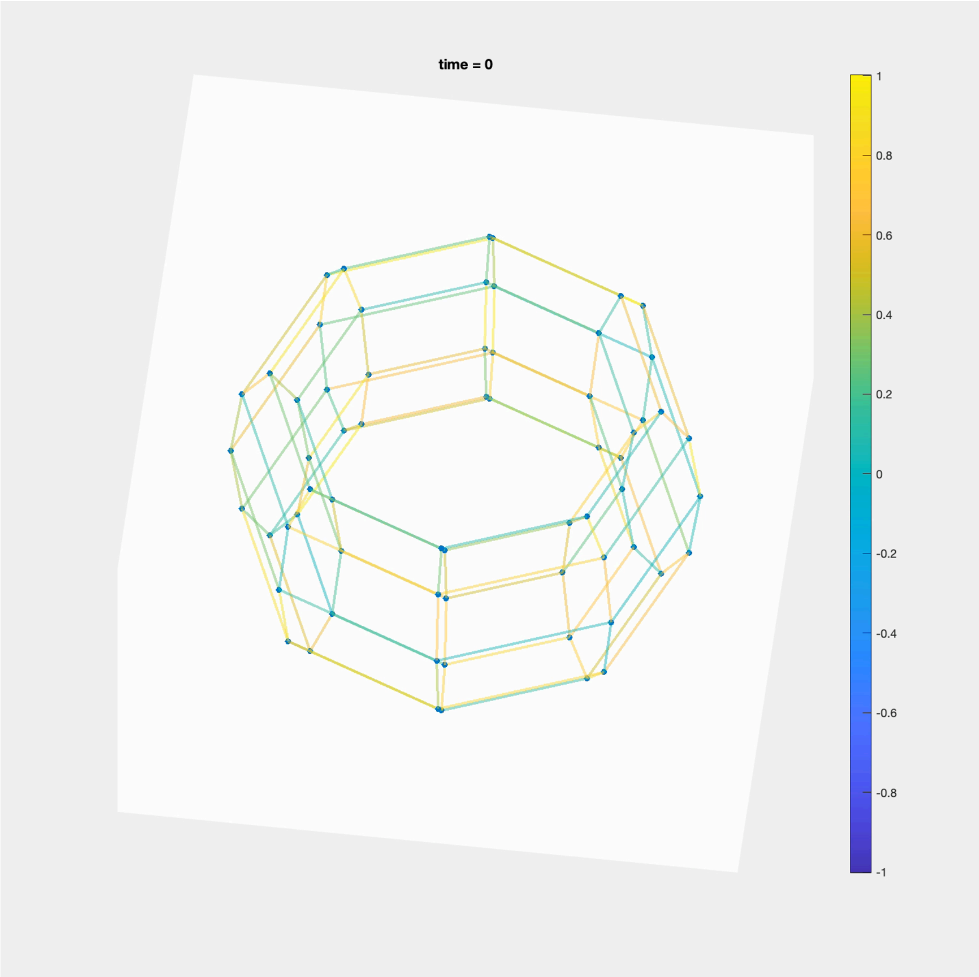

Which are the topological and dynamical conditions under which we can observe Global Topological Synchronization?

For example all the edges displaying the same dynamics?

Carletti, Giambagli Bianconi
PRL 2023

Wang, Muolo, Carletti, Bianconi
PRE 2024

Cell complexes

(a) (b) (c) (d) (e)

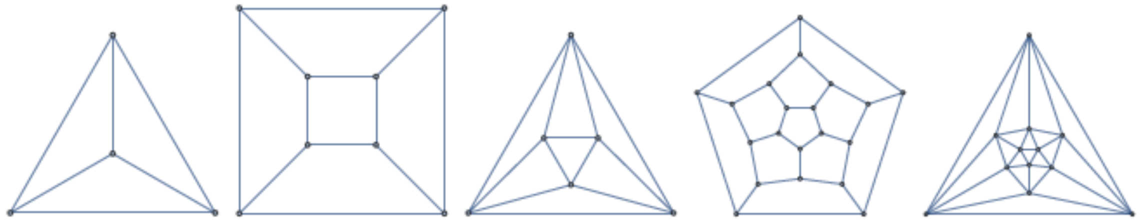

(a) (b) (c) (d) (e)

A cell complex $\hat{\mathcal{K}}$ has the following two properties:

(a) it is formed by a set of cells that is closure-finite, meaning that every cell is covered by a finite union of open cells;

(b) given two cells of the cell complex $\alpha \in \hat{\mathcal{K}}$ and $\alpha' \in \hat{\mathcal{K}}$ then either their intersection belongs to the cell complex, i.e. $\alpha \cap \alpha' \in \hat{\mathcal{K}}$ or their intersection is a null set, i.e. $\alpha \cap \alpha' = \emptyset$.

Coupled identical topological signals

- Let $\mathbf{x}_r$ indicate a topological signal

- The coupled dynamics obeys

$$\frac{d\mathbf{x}_r}{dt} = \mathbf{f}(\mathbf{x}_r) - \sigma \sum_{\beta} [L_{[n]}]_{rq}\, \mathbf{h}(\mathbf{x}_q)$$

- In order to ensure eqivariance, i.e. invariance under change of orientation of the simplices $\mathbf{f}(\mathbf{x}), \mathbf{h}(\mathbf{x})$ should be **odd** functions.

Properties of global synchronization of topological signals

- The globally synchronised state is aligned with an harmonic eigenvector of the Hodge Laplacian
- Harmonic eigenvectors are localised on holes.
- **Global synchronisation requires topologies with holes that span the entire simplicial or cell complex**.

Carletti, Giambagli, Bianconi (2023)

Example of manifolds sustaining global synchronisation

Synchronisation of $(n-1)$-dimensional topological signal

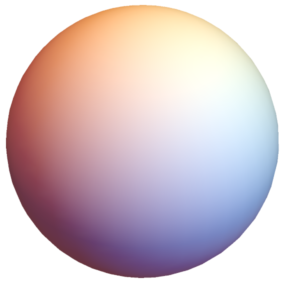

n-dimensional hypersphere

Betti numbers

$$\beta_0 = \beta_{n-1} = 1$$
$$\beta_k = 0 \text{ for } 0 < k < n-1$$

Synchronisation of any k-dimensional topological signal

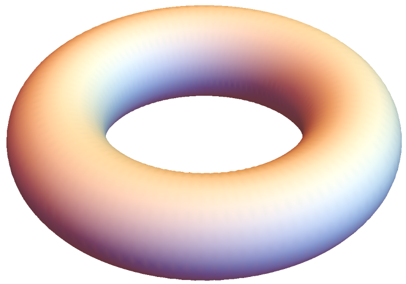

n-dimensional torus (cell complex)

Betti numbers

$$\beta_k = \binom{n-1}{k}$$

Global topological synchronization of unweighted d-dimensional Tori

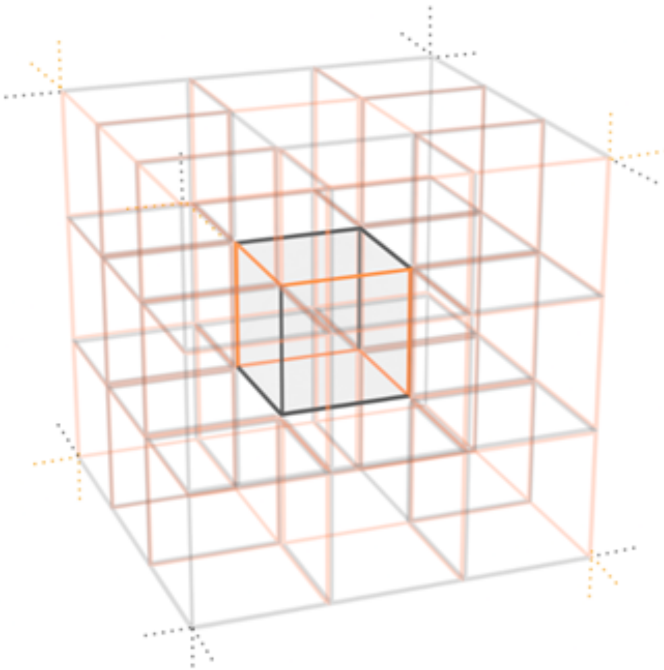

d-dimensional Tori admit,

under suitable dynamical conditions,

global synchronization of any

m-dimensional topological signal with

$$0 \leq m \leq d$$

Global Topological Synchronisation

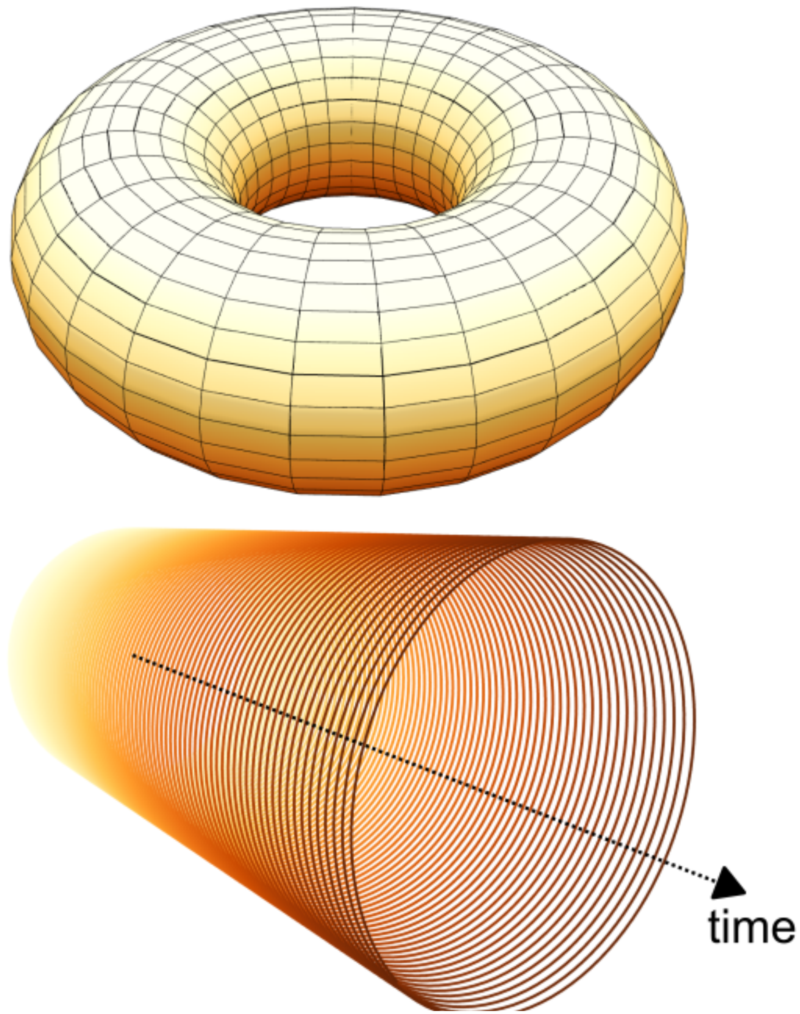

Processing topological signals

How can we treat and process topological signals of different dimension together?

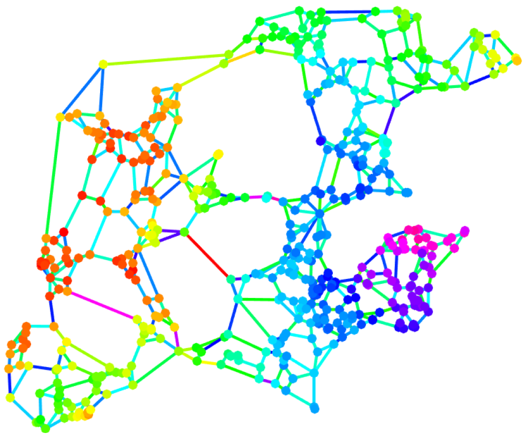

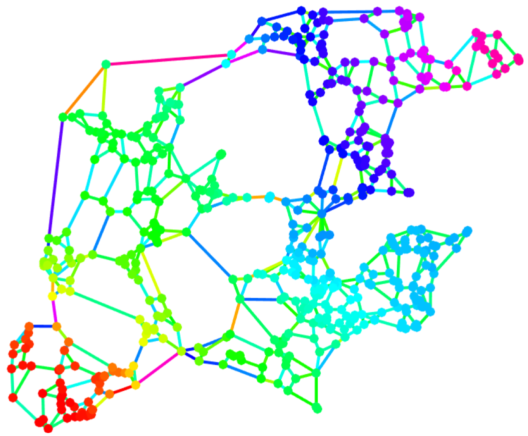

G. Bianconi,
Topological Dirac equation on networks and simplicial complexes JPhys Complexity (2021)

Dirac legacy

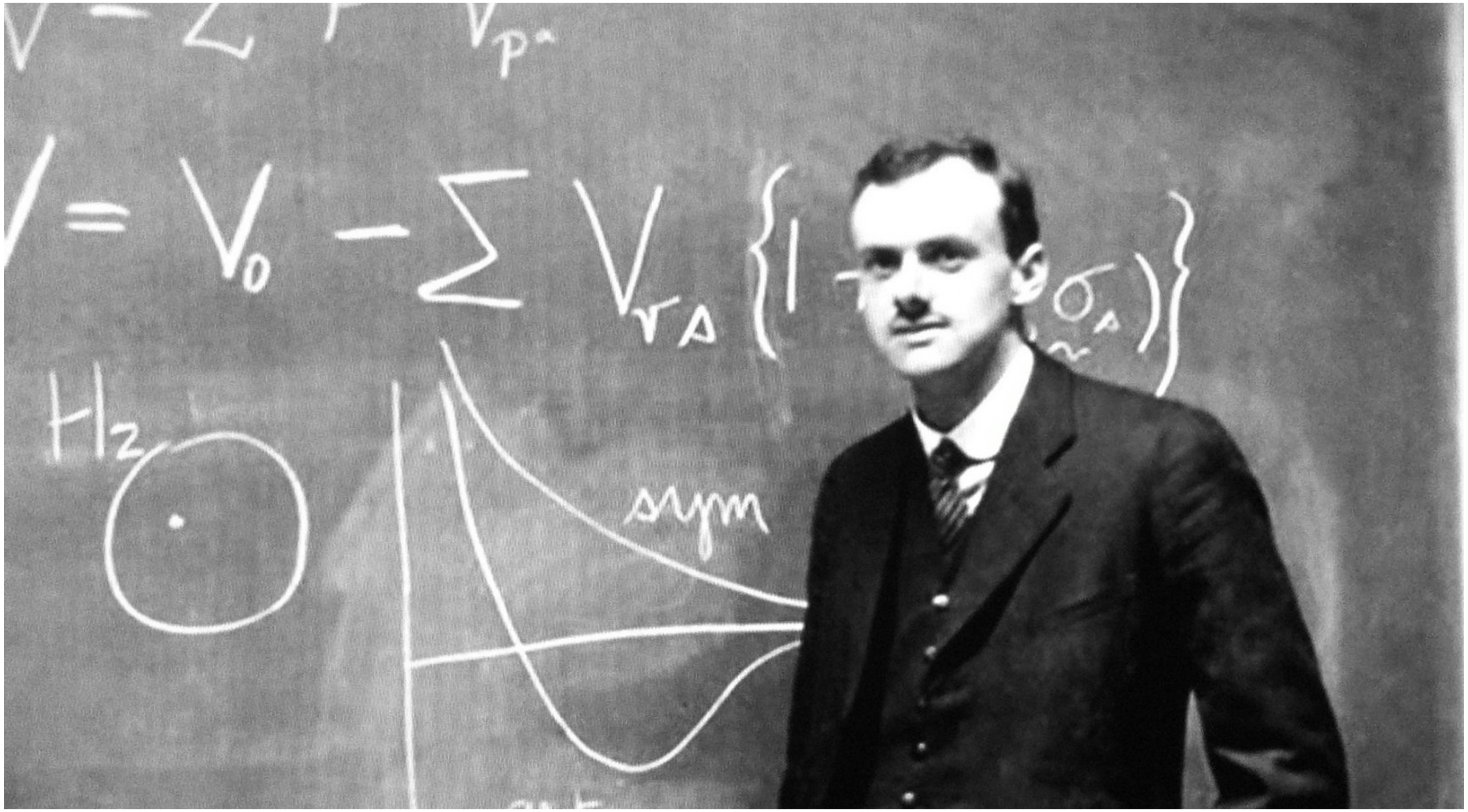

The Dirac operator of simplicial complexes

**The Dirac operator allows
to study interacting topological signals of different dimensions
coexisting in the same network topology**

Dirac operator

$$\mathbf{D} = \begin{pmatrix} 0 & \mathbf{B}_1 & 0 \\ \mathbf{B}_1^\top & 0 & \mathbf{B}_2 \\ 0 & \mathbf{B}_2^\top & 0 \end{pmatrix},$$

Topological signal "spinor"

$$\mathbf{s} = \begin{pmatrix} \chi \\ \psi \\ \xi \end{pmatrix}$$

χ **Node signal**

ψ **Link signal**

ξ **Triangle signal**

The action of the Dirac operator

In signal processing, the Dirac operator allows cross-talking between signals of different dimension

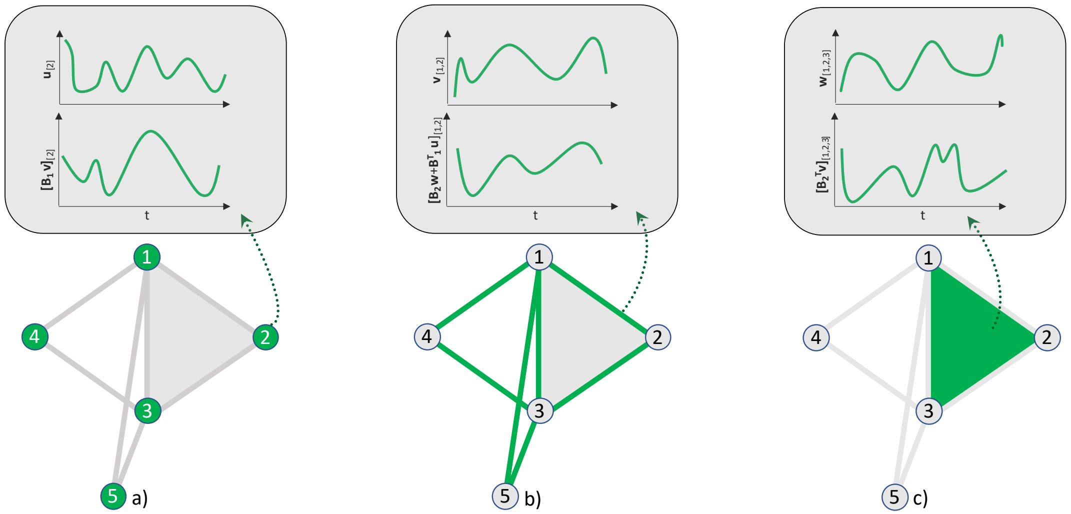

$$\mathbf{D} = \begin{pmatrix} 0 & \mathbf{B}_1 & 0 \\ \mathbf{B}_1^\top & 0 & \mathbf{B}_2 \\ 0 & \mathbf{B}_2^\top & 0 \end{pmatrix}, \text{ acts on } \boldsymbol{\Psi} = \begin{pmatrix} \chi \\ \psi \\ \xi \end{pmatrix} \quad \rightarrow \quad \mathbf{D}\boldsymbol{\Psi} = \begin{pmatrix} \mathbf{B}_1\psi \\ \mathbf{B}_1^\top\chi + \mathbf{B}_1\xi \\ \mathbf{B}_2^\top\psi \end{pmatrix}$$

The Dirac as the square-root of the Laplacian

The Dirac operator
can be interpreted as the
“square-root” of the Laplacian

$$\boldsymbol{D} = \begin{pmatrix} 0 & \mathbf{B}_1 & 0 \\ \mathbf{B}_1^\top & 0 & \mathbf{B}_2 \\ 0 & \mathbf{B}_2^\top & 0 \end{pmatrix}, \text{ acts on } \boldsymbol{\Psi} = \begin{pmatrix} \chi \\ \psi \\ \xi \end{pmatrix} \quad \rightarrow \quad \mathbf{D}^2 = \mathscr{L} = \begin{pmatrix} \mathbf{L}_{[0]} & \mathbf{0} & \mathbf{0} \\ \mathbf{0} & \mathbf{L}_{[1]} & \mathbf{0} \\ \mathbf{0} & \mathbf{0} & \mathbf{L}_{[2]} \end{pmatrix}$$

Topological Dirac equation

G. Bianconi,
Topological Dirac equation on networks and simplicial complexes
JPhys Complexity (2021)

Topological Dirac equation

The topological Dirac equation is then given by

$$i\partial_t \mathbf{\Psi} = \mathscr{H}\mathbf{\Psi}$$

with Hamiltonian

$$\mathscr{H} = \mathbf{D} + m\boldsymbol{\beta}$$

Where $\mathbf{\Psi} = \begin{pmatrix} \boldsymbol{\chi} \\ \boldsymbol{\psi} \end{pmatrix}$ and $\boldsymbol{\beta} = \begin{pmatrix} \mathbf{1} & \mathbf{0} \\ \mathbf{0} & -\mathbf{1} \end{pmatrix}$

leading to the anti-commutator $\{\mathbf{D}, \boldsymbol{\beta}\} = \mathbf{0}$

Energy Eigenstates

The energy eigenstates satisfy $E\mathbf{\Psi} = \mathscr{H}\mathbf{\Psi}$

which leads to

$$E\boldsymbol{\chi} = \mathbf{B}\boldsymbol{\psi} + m\boldsymbol{\chi},$$
$$E\boldsymbol{\psi} = \mathbf{B}^{\top}\boldsymbol{\chi} - m\boldsymbol{\psi}$$

$\boldsymbol{\chi}, \boldsymbol{\psi}$ are respectively the singular vectors of $\mathbf{B}$

with singular value λ and the energy E

is given by $E = \pm\sqrt{|\lambda|^2 + m^2}$

Matter-Antimatter asymmetry and homology

For $E^2 > m^2$ there is symmetry between positive energy eigenstates and negative energy eigenstates.

However the symmetry between positive energy states and negative energy states breaks down for $|E| = m$

The states at energy states at $E = m$ are localised on nodes and they have a degeneracy given by the Betti number β_0

The energy states $E = -m$ are localised on links and they have a degeneracy given by the Betti number β_1

Dirac equation spectrum and eigenstate

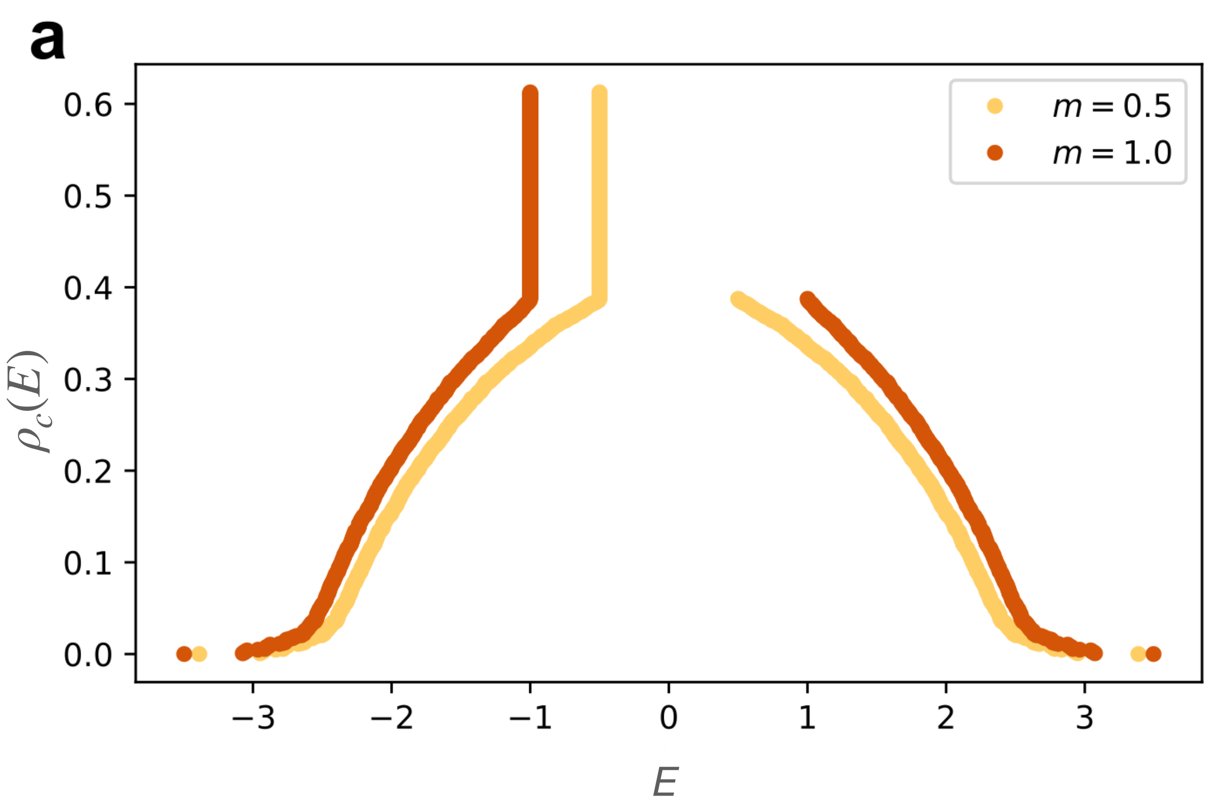

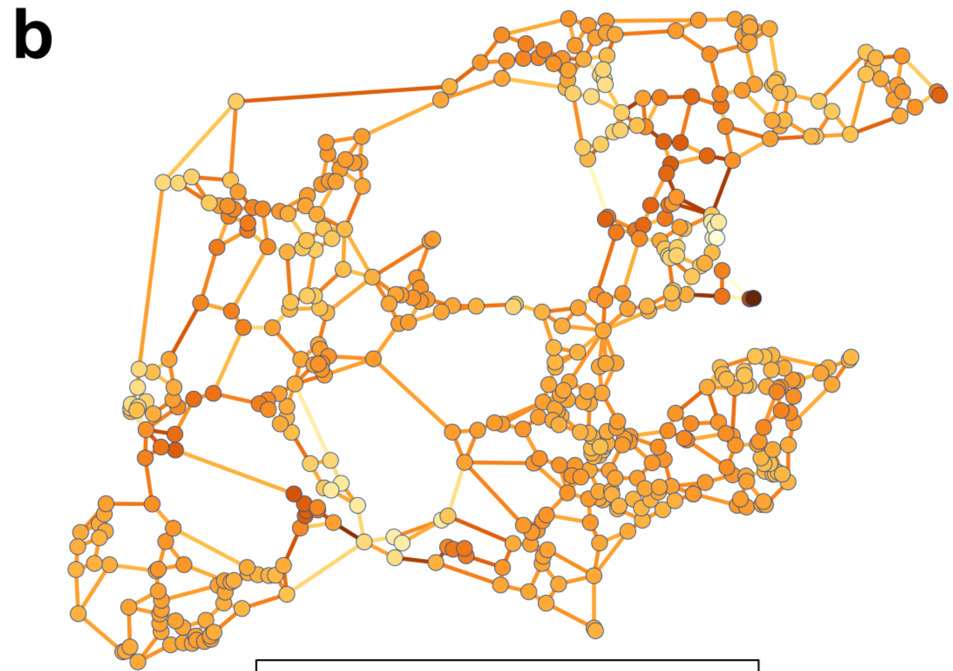

$$\boxed{\mathrm{i}\partial_t \boldsymbol{\Psi} = (\mathbf{D} + \boldsymbol{\gamma}_0 m)\boldsymbol{\Psi}}$$

Nambu-Jona Lasinio legacy

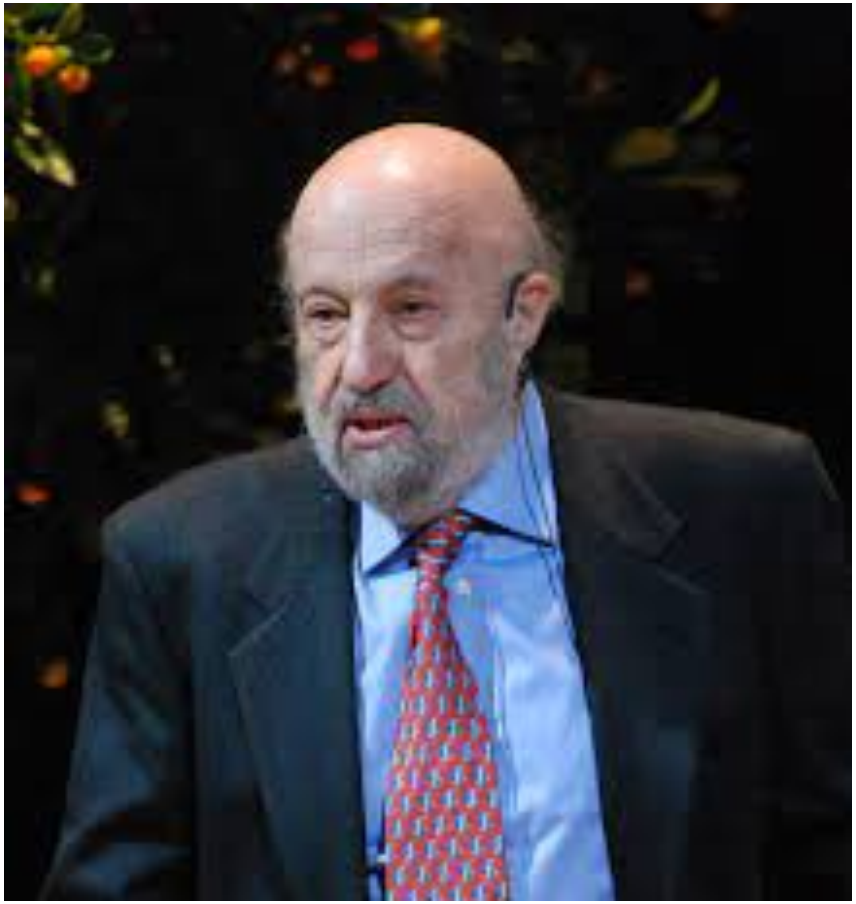

Mass of simple and higher-order networks

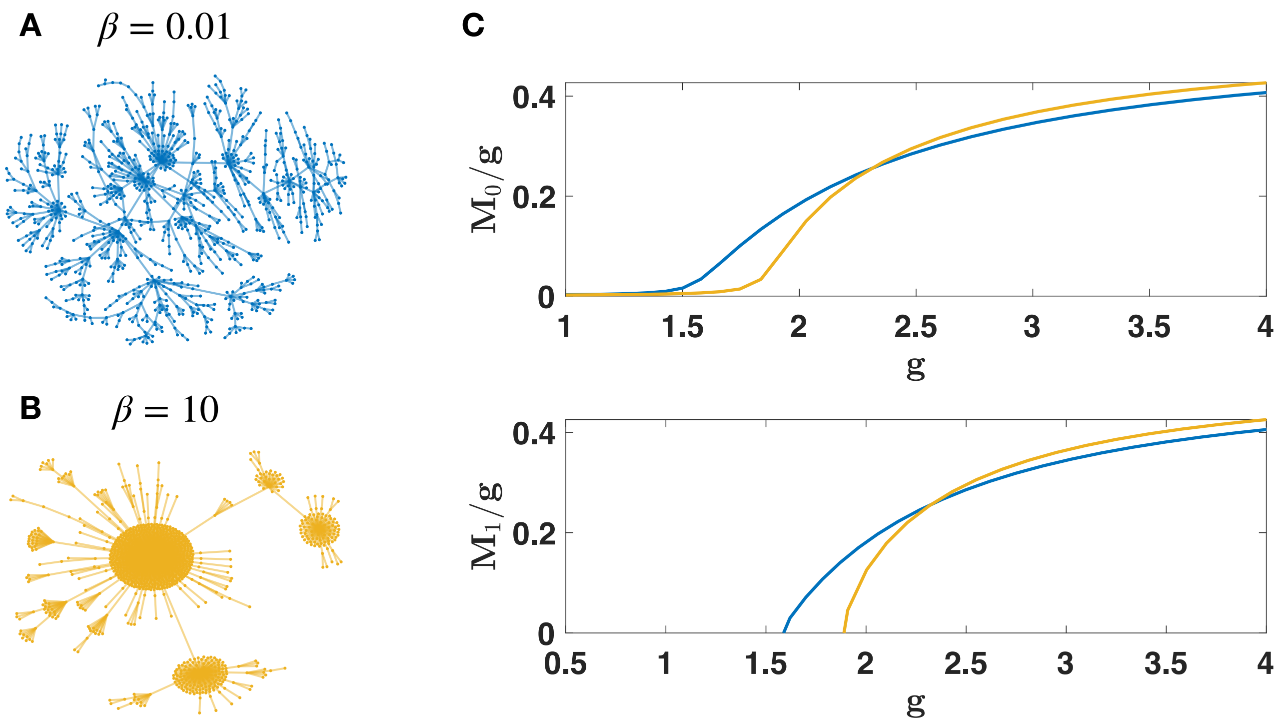

Gap equation

$$M_0 = \frac{g}{\mathcal{N}} \sum_{i=1} \beta_{2i} + \frac{g}{\mathcal{N}} \sum_{\lambda>0} \frac{M_0}{\sqrt{M_0^2 + \lambda^2}}$$

$$M_1 = \frac{g}{\mathcal{N}} \sum_{i=1} \beta_{2i+1} + \frac{g}{\mathcal{N}} \sum_{\lambda>0} \frac{M_1}{\sqrt{M_1^2 + \lambda^2}}$$

The mass of simple or higher-order networks depends on their geometry and topology

G. Bianconi The mass of simple and higher-order networks JPhysA (2023)

Mass of a random network

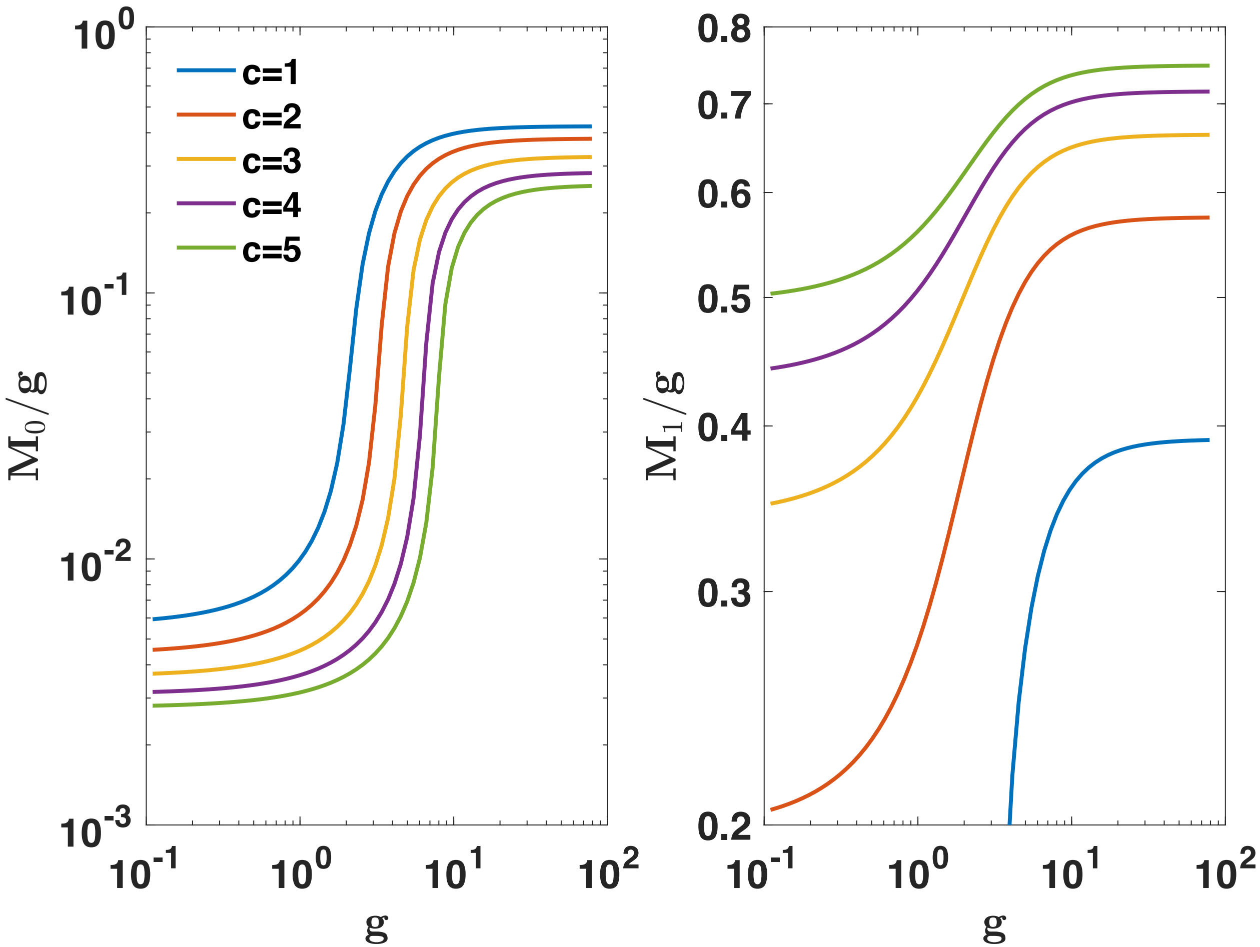

The mass of the giant component of a random Erdos-Renyi graph with average degree c

Dependence on the mass on the network geometry

Changing the geometry

of the network by considering

non trivial metric matrices

changes the mass of the network

Here comparing the mass of the weighted

and unweighted collaboration network

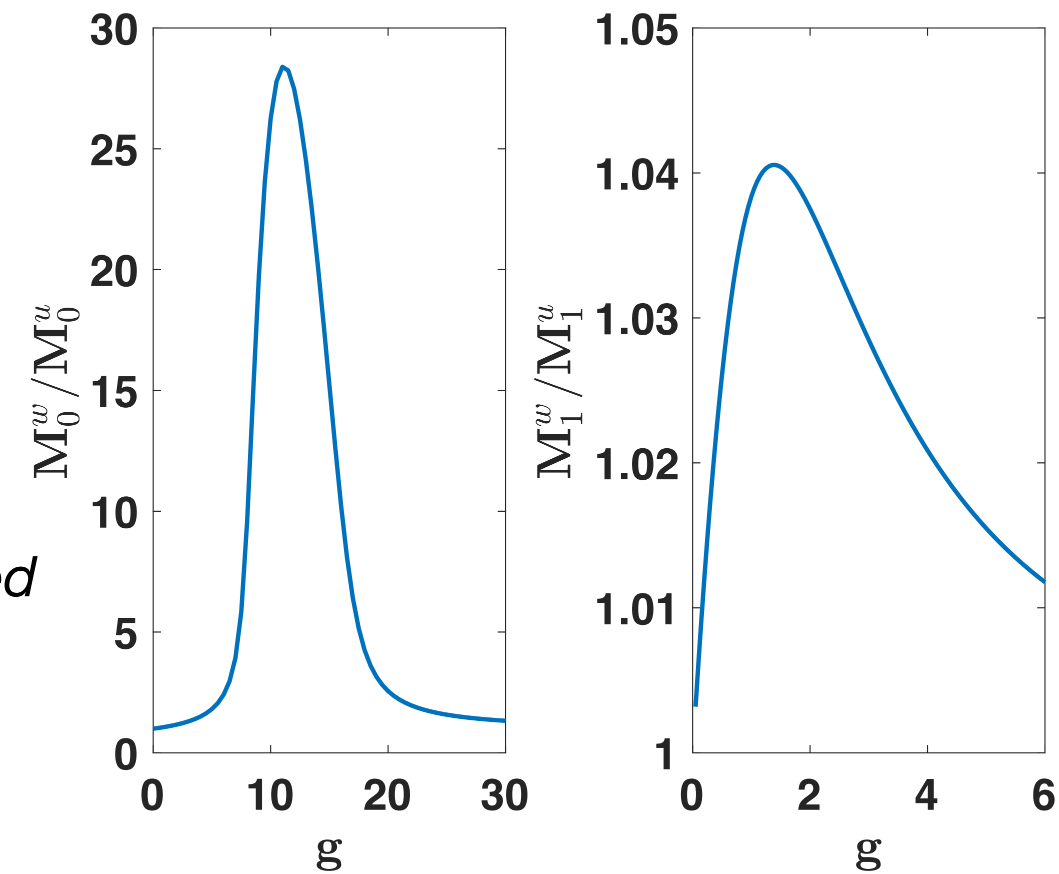

G. Bianconi The mass of simple and higher-order networks JPhysA (2023)

Dirac operator

and

Complexity

Coupling topological signals of different dimension

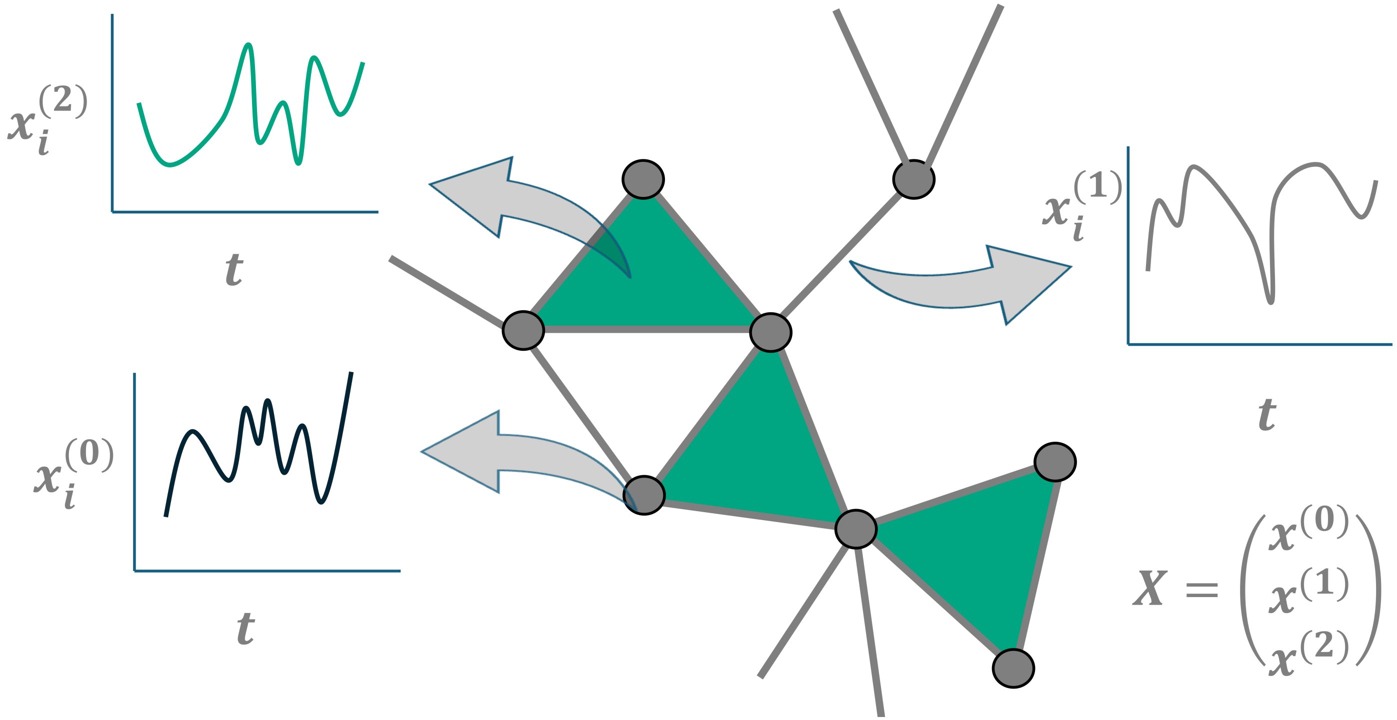

Dirac operator
In complex systems

Dirac synchronisation:
Synchronisation involving node and edge topological signals entangled with each other.
The dynamical order involves many minima corresponding with the multiple harmonic eigenvector of the network or simplicial complex
(Communication Physics 2022, Chaos 2023)

Dirac Turing patterns:
Node and edge topological signal can give rise to dynamical instabilities and Dirac pattern formation
(PRE 2022, Chaos Solitons and Fractals 2024)

Global Topological Dirac Synchronization:
The Dirac operator can be used to couple identical oscillators on simplices of different dimensions
(arxiv preprint 2024)

Dirac Signal Processing

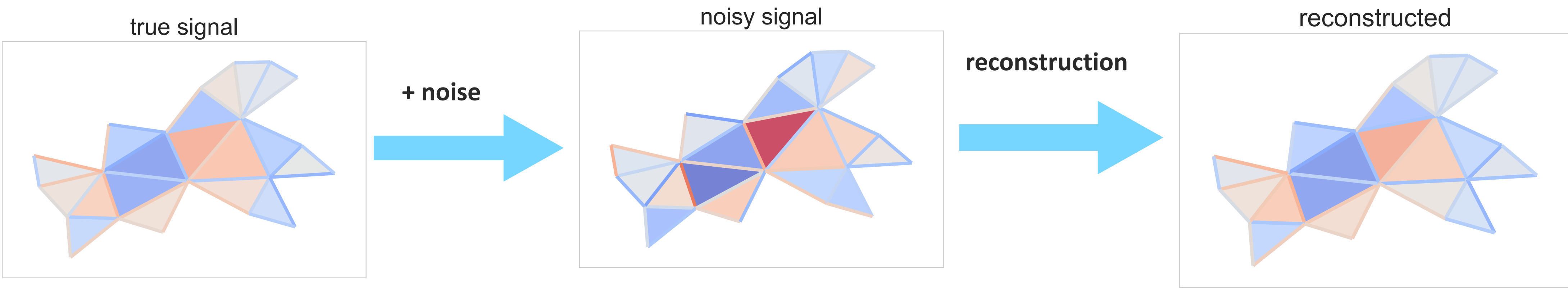

The Dirac operator allows us to filter out nodes and links signals **jointly**

L. Calmon, M. Schaub and G. Bianconi (2023)
R. Wang, Y. Tian, P. Lio, G. Bianconi (2024)

Dirac-Equation Signal Processing

Given a **noisy topological signal defined on both nodes and edges**

$\tilde{\boldsymbol{\psi}} = \boldsymbol{\psi} + \boldsymbol{\epsilon}$ with $\boldsymbol{\epsilon}$ noise

Joint-filtering with the Dirac:

$$\mathscr{L} = \|\tilde{\boldsymbol{\psi}} - \hat{\boldsymbol{\psi}}\|_2^2 + \gamma \hat{\boldsymbol{\psi}}^T \left(\mathbf{D} + m\boldsymbol{\gamma} - E\mathbf{I}\right)^2 \hat{\boldsymbol{\psi}}$$

$E = m = 0$ Hodge Laplacian kernel

$m = 0, E \neq 0$ Dirac signal processing

$m \neq 0, E \neq 0$ Dirac-equation signal processing

The parameters E and m can be learned from data

Dirac-Equation Signal Processing

Eigenstates of the Topological Dirac equation with mass m=1.5

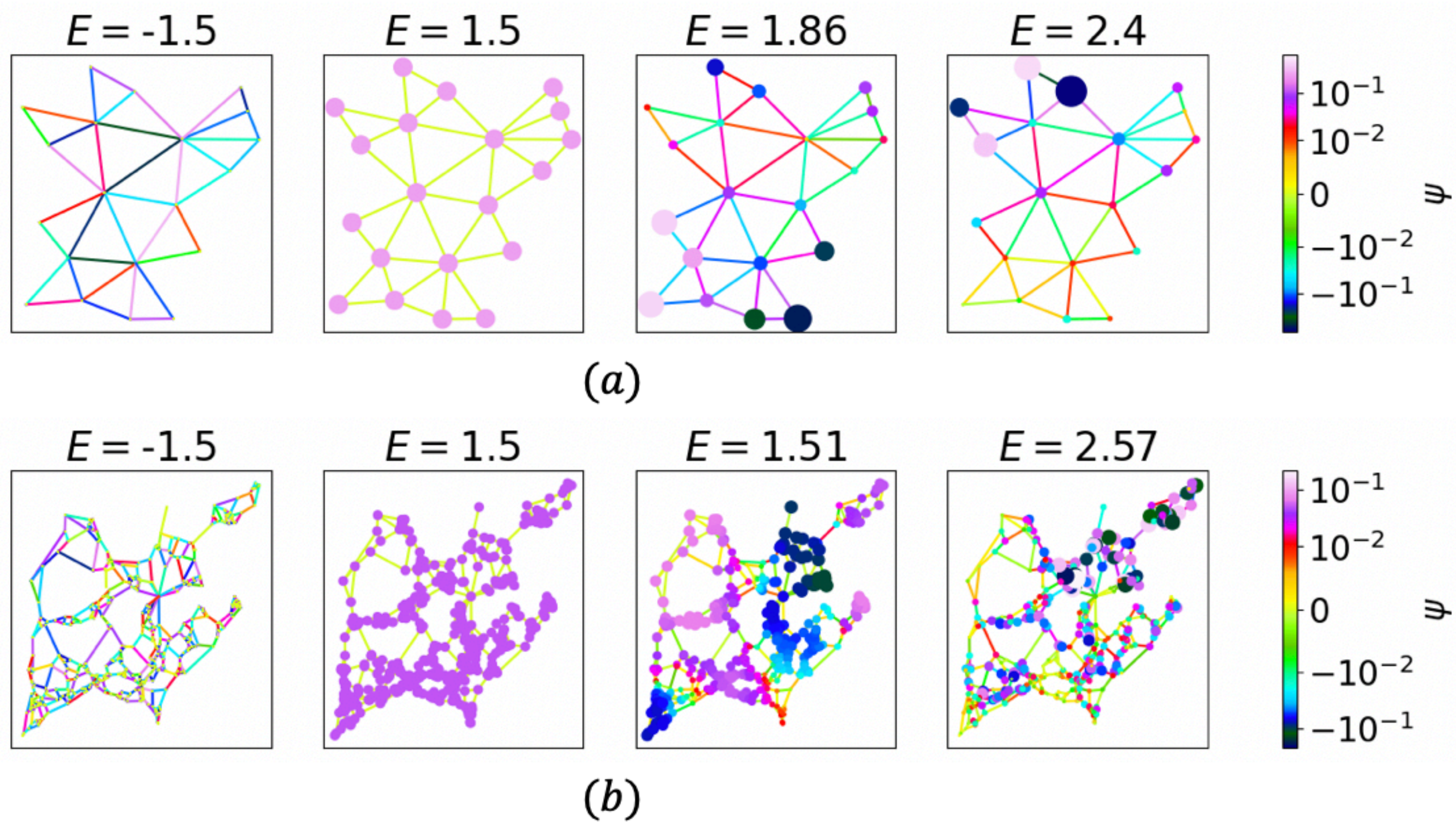

The Iterated Dirac-equation signal processing (IDESP) on real data

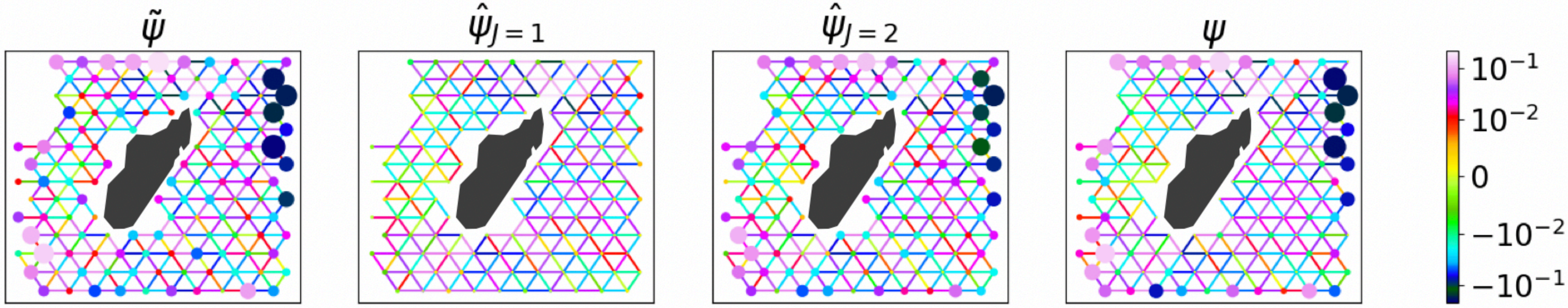

Noisy signal **First iteration of IDESP** **Second iteration of IDESP** **True data**

The IDESP can reconstruct real signal on nodes and edges

It outperform the Hodge Laplacian signal processing (LSP) if the true signal is not harmonic

It reduces to the Hodge Laplacian signal processing if the signal is almost harmonic

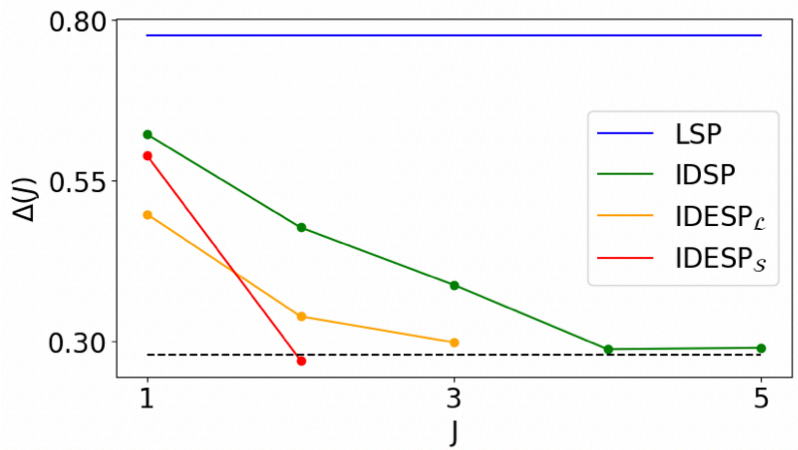

Dirac persistent homology: Application to Biomolecules

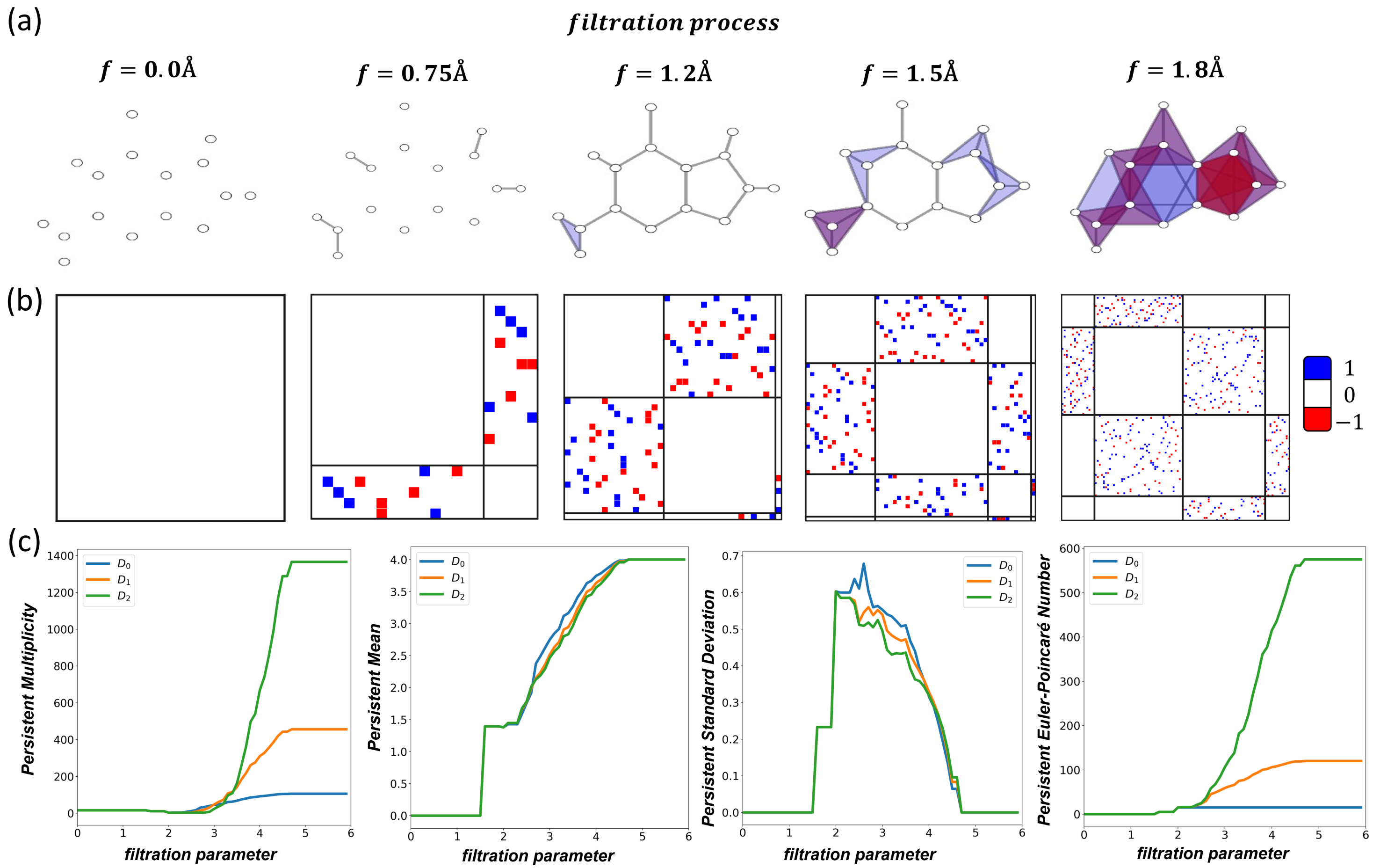

Wee et al. (2023)

Classification of molecules with Persistent Dirac

Wee et al. (2023)

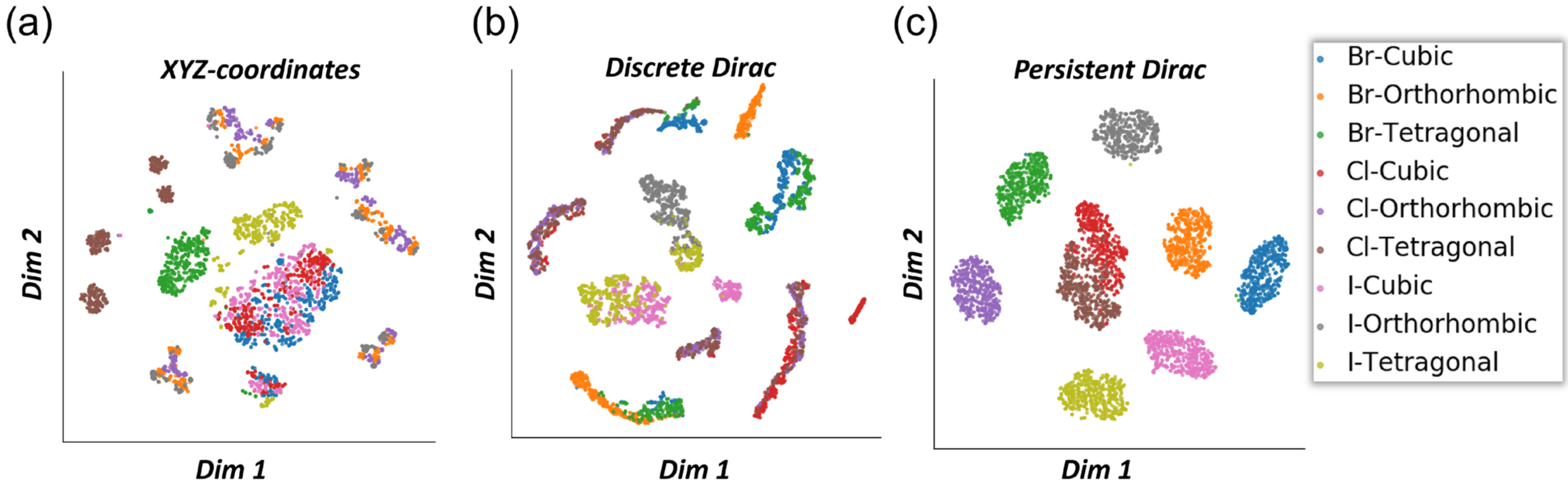

Dirac-based Gaussian kernel

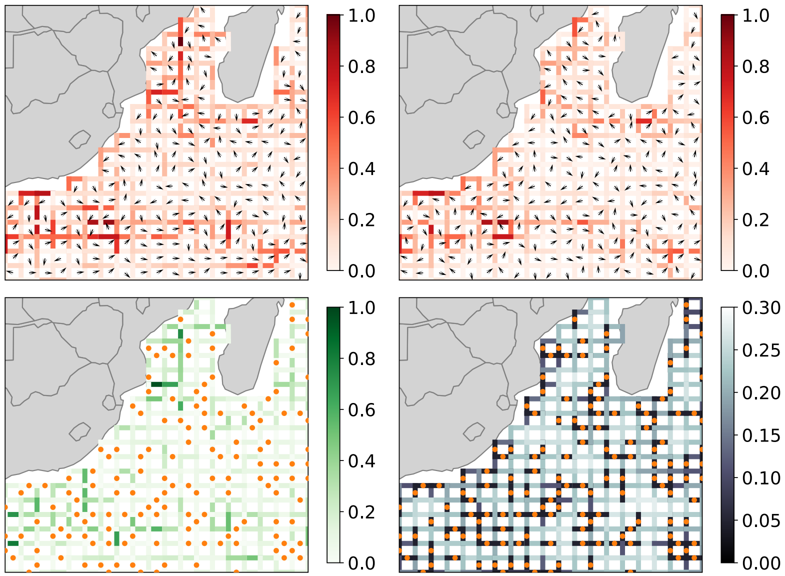

$$\mathcal{D} = \begin{pmatrix} \mathbf{0} & \mathbf{B}_1 & \cdots & \mathbf{0} \\ \mathbf{B}_1^\top & \ddots & \ddots & \vdots \\ \vdots & \ddots & \ddots & \mathbf{B}_n \\ \mathbf{0} & \cdots & \mathbf{B}_n^\top & \mathbf{0} \end{pmatrix},$$

$$(r\mathbf{I} - c\mathcal{D} + d\mathcal{L})^{\frac{\nu}{2}} \boldsymbol{f} = \boldsymbol{w}, \quad \boldsymbol{w} \sim \mathcal{N}(0, \mathbf{I})$$

Mathieu A., So T., Brooks P., and Deisenroth M. P..
Gaussian Processes on Cellular Complexes
In International Conference on Machine Learning, 2024

Simplicial Attention Neural Networks based on Dirac decomposition

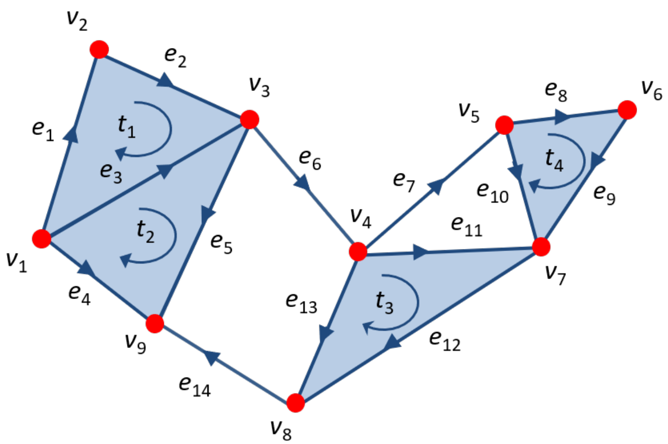

$$\mathbf{D}_{\mathcal{X}} = \begin{bmatrix} \mathbf{0} & \mathbf{B}_1 & \mathbf{0} \\ \mathbf{B}_1^T & \mathbf{0} & \mathbf{B}_2 \\ \mathbf{0} & \mathbf{B}_2^T & \mathbf{0} \end{bmatrix}. \tag{12}$$

Due to its structure, it can be easily shown that a Dirac decomposition similar to the Hodge decomposition in (10) holds [42]. In particular, for a simplicial complex $\mathcal{X}_2$ of order two, the Dirac decomposition is given by:

$$\mathbb{R}^{N+E+T} = \text{im}(\mathbf{D}_{\mathcal{X}}^{(d)}) \oplus \text{im}(\mathbf{D}_{\mathcal{X}}^{(u)}) \oplus \ker\big(\mathbf{D}_{\mathcal{X}}\big), \tag{13}$$

where:

$$\mathbf{D}_{\mathcal{X}}^{(d)} = \begin{bmatrix} \mathbf{0} & \mathbf{B}_1 & \mathbf{0} \\ \mathbf{B}_1^T & \mathbf{0} & \mathbf{0} \\ \mathbf{0} & \mathbf{0} & \mathbf{0} \end{bmatrix}, \quad \mathbf{D}_{\mathcal{X}}^{(u)} = \begin{bmatrix} \mathbf{0} & \mathbf{0} & \mathbf{0} \\ \mathbf{0} & \mathbf{0} & \mathbf{B}_2 \\ \mathbf{0} & \mathbf{B}_2^T & \mathbf{0} \end{bmatrix}. \tag{14}$$

Battiloro, C., Testa, L., Giusti, L., Sardellitti, S., Di Lorenzo, P. and Barbarossa, S., 2024.
Generalized simplicial attention neural networks.
IEEE Transactions on Signal and Information Processing over Networks.

Dirac-Bianconi Graph Neural Networks-Enabling long-range graph predictions

Topological Dirac equation neural network

$$i\partial_t \begin{pmatrix} x(t) \\ e(t) \end{pmatrix} = \left(\partial_{DB} + \begin{pmatrix} \beta & 0 \\ 0 & -\beta \end{pmatrix}\right) \begin{pmatrix} x(t) \\ e(t) \end{pmatrix} \quad (8)$$

$$= (\partial_{DB} + \boldsymbol{W}_\beta) \begin{pmatrix} x(t) \\ e(t) \end{pmatrix} . \quad (9)$$

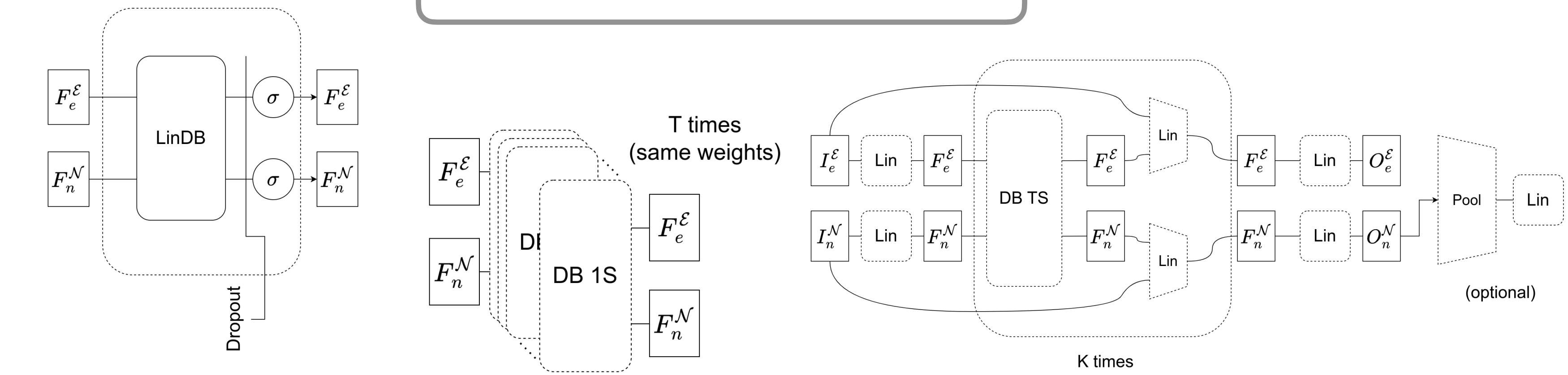

(a) Dirac Bianconi 1-Step (DB1S) (b) Dirac Bianconi T-Step (c) DBGNN layer, where Lin denotes a linear layer.

Nauck, C., Gorantla, R., Lindner, M., Schürholt, K., Mey, A.S. and Hellmann, F. 2024, Dirac--Bianconi Graph Neural Networks-Enabling long-range graph predictions. In *ICML 2024 Workshop on Geometry-grounded Representation Learning and Generative Modeling*.

Conclusions

Network theory
unveils the interplay between network topology and dynamics
in complex systems with applications
to brain research, theoretical physics and AI

Higher-order networks reveal how topology shapes dynamics.
(PRL 2020, Communications Physics 2021,PRL 2023)

The Dirac operator is key to build a fundamental
theory of networks
(JPhys Complexity 2021, Communications Physics 2022,
JPhysA 2023,New Journal of Physics 2023)

The new physics challenge
is to combine statistical mechanics and information theory
with our novel understanding of
the role of network topology and geometry
to shape the dynamics of complex systems

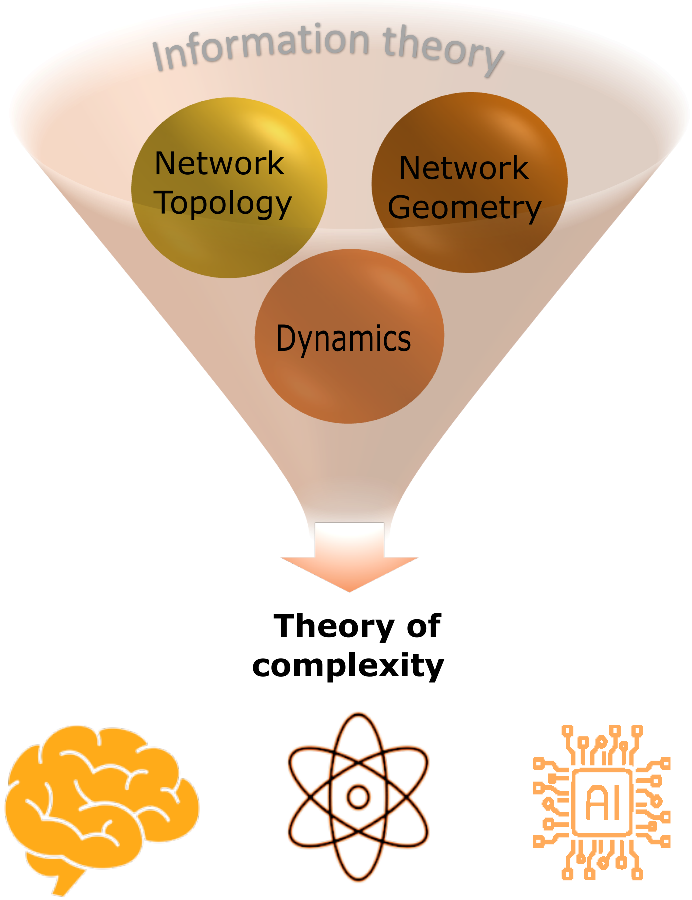

Collaborators

Ginestra Bianconi Lab at QMUL

- Runyue Wang
- Marta Niedostatek
- Hanlin Sun (now at NORDITA)
- Lucille Calmon (Now at Sorbonne University)
- Ana Paula Millan (now at Granada University)

Codes Available at

External Collaborators

- Timoteo Carletti (Namur University)
- Lorenzo Giambagli (Freie Universität of Berlin)
- Juergen Kurths (PIK)
- Pietro Lio (Cambridge University)
- Riccardo Muolo (Institute of Science Tokyo)
- Filippo Radicchi (Indiana University)
- Juan Restrepo (Colorado University)
- Michael Schaub (Aachen University)
- Yu Tian (Max Planck, Dresden)
- Joaquin Torres (Granada University)
- Kelin Xia (Nangyang Technical University, SG)

Queen Mary
University of London